A Proposed

TRIAXIAL DIGITAL FLUXGATE MAGNETOMETER

FOR NASA APPLICATIONS EXPLORER MISSION:

RESULTS OF TESTS OF CRITICAL ELEMENTS

M.G. McLeod

J.D. Means

April 1977

Table of Contents

Figures

Introduction:

This report describes some tests performed to prove the critical elements of the triaxial digital fluxgate magnetometer design described in the interim report by McLeod, 1976 (reference 1).

The performance of the unit tested was outstanding. The temperature stability of gain and zero offset were better than for any other fluxgate magnetometer of which the writer is aware. A major reason for this excellent performance is the use of an autocalibration feature (or "chopper stabilization").

A novel method for improving the linearity of the analog to digital converter portion of the instrument proved successful. This feature is described in detail in the interim report (reference 1). It involves adding a sawtooth waveform to the signal being measured before the A/D conversion, and averaging the digital readings over one cycle of the sawtooth. It is intended to reduce "bit error" nonlinearities present in the A/D converter which could be expected to be as much as 16 gamma if not reduced. No such nonlinearities were detected in the output of the instrument which included the feature designed to reduce these nonlinearities. However, a small scale nonlinearity of $\pm$ 2 gamma with a 64 gamma repetition rate was observed in the unit tested. A design improvement intended to eliminate this small scale nonlinearity is described in the body of this report.

The analog magnetometer worked well. The use of a chopper stabilized op amp to supply feedback current to the sensor proved successful. The use of a separate reference ground brought out from the chopper op amp to the multiplexer proved beneficial. This feature was intended to reduce problems

with ground loops. If the analog ground on the breadboard containing the chopper op amp were used in place of the reference ground; a zero offset error of approximately 40 gamma would have been introduced.

A number of problems were isolated when the unit was first tested, and circuit modifications were made to solve these problems. The problems and the circuit modifications are described in the body of this report. Time limitations precluded making the modification to eliminate the small scale nonlinearity discussed previously.

The unit tested meets most of the very stringent Magsat specifications; however, noise was greater than specified. The writer believes that the modification to eliminate the small scale nonlinearity would reduce this noise appreciably. This modification and tests to verify its efficacy are highly recommended.

The interim report (reference 1) should be consulted for a detailed description of the operation of the instrument and calculations of the performance parameters that the instrument could be expected to meet. The writer believes that with the recommended improvement the instrument would meet these calculated performance parameters.

Description of Test Program:

The test program consisted of the following steps:

1. Design of digital interface circuitry so that the magnetometer can be controlled and the digital outputs processed by a Hewlett Packard HP21MX minicomputer system. A microprocessor would be used in place of the minicomputer in a completed design.

2. Completion of detailed design and parts layout of remaining circuitry.

3. Construction of breadboard prototype.

4. Debugging of prototype. Correction of wiring errors and omissions.

5. Programming minicomputer to operate the magnetometer.

6. Stability, offset, crosstalk, linearity, and temperature sensitivity measurements.

7.   Identification of problems and tests to isolate source of problems. Modifications of circuits to reduce the problems where possible.

8.   Repetition of tests on modified circuitry.

9.   Preparation of report with recommendations for improvements.

The magnetometer system design and some of the detailed circuitry used are given in the interim report by McLeod, 1976. The single axis magnetometer tested consisted of four individual breadboard circuits which were plugged into an interface connector box. Also connected to the interface box were the sensor cable and a cable from the minicomputer together with power supply connections. The four breadboard circuits were:

1.   Drive circuit.

2.   Second harmonic amplifier.

3.   Output board, consisting of integrator lowpass filter, and current feedback amplifier.

4.   Digital board, consisting of a multiplexer, A/D converter and associated parts, and the digital circuits required to interface with the minicomputer.

The first two breadboards were modified versions of boards used in the construction of other UCLA magnetometers. A schematic diagram for the third board (the output board) is given in Appendix A, while a schematic diagram for the digital board is given in Appendix B.

Summary of Test Results:

Several problems were isolated and the circuits modified from those given in the interim report as discussed below:

1.   It was found that in addition to the second harmonic signal proportional to the magnetic field component along the sensor magnetic axis present at the

sensor sense winding, there was also present a second harmonic component 90° out of phase with this signal and proportional to the magnetic field component in a direction normal to the magnetic axis and roughly in the plane of the ring core. This second component was approximately one tenth of one percent of the first component for the same size field component. In order that this second component, which was not reduced nearly to zero at the second harmonic amplifier output like the first component by the feedback, not cause "clipping" in the second harmonic amplifier, it was thought to be desirable to reduce the gain of this amplifier by a factor of ten relative to the value originally chosen. This was accomplished by changing the one megohm resistors associated with the integrator and shown in Figure 5 of the interim report to 100K, and choosing the feedback resistors shown in Figure 4 of that report as "to be selected" to have the value 340K. This change would result in an increase of the maximum slew rate to one million gamma per second, and an increase in the offset and offset drift due to the integrator by a factor of ten. Since the resulting offset drift would still be only ten percent of that due to the rest of the instrument, the instrument performance would not be noticably impaired by this change.

It should be noted that the quadrature component mentioned would not be present if the actual sensor had the perfect symmetry of the design. Therefore, the size of this quadrature component can be expected to vary markedly from one sensor to another.

2. It was found that digital signals were present on the reference analog ground line shown in Figure 6 of the interim report and interfered with the operation of the chopper feedback amplifier, resulting in a field offset of approximately fifteen gamma due to this effect. This offset was substantially eliminated by connecting a 0.75 μF capacitor between the positive op amp input and analog ground (capacitor C19 shown in Appendix A).

3. It was found that a signal at the fundamental frequency and its harmonics was present across the feedback winding. (A similar signal is present across the sense winding). This signal interacted with the chopper feedback amplifier in a nonlinear fashion to produce second harmonic signal, which was applied to the feedback winding, and which produced an offset of about fifteen gamma. This offset was reduced below 0.01 gamma by (a) inserting a resistor (R16 shown in Appendix A) in series with capacitor C12 to increase the input impedance to the chopper op amp at the second harmonic frequency and thus reduce the amount of second harmonic current applied to the feedback winding, and by (b) using a more effective filter (shown in Appendix A) to filter second harmonic from the feedback winding.

4. A nonlinearity was observed in the composite A/D converter. It was found that when a voltage corresponding to 40,000 gamma was applied to the multiplexer input in place of the magnetometer signal, the digital output magnitude changed by an amount corresponding to 35 gamma when the polarity of the applied voltage was reversed. This nonlinearity was found to be due to a low (and nonlinear) common mode rejection for the Burr Brown 3550K op amp used in the voltage follower. This op amp and the one used in the adder were changed to Burr Brown 3506 J op amps which have higher common mode rejection and a higher useful range of common mode voltage. A 100pF compensation capacitor was used with the voltage follower op amp. This change reduced the previous 35 gamma difference in readings when the input voltage polarity was reversed to less than one gamma. It also reduced the gain temperature sensitivity of the composite converter.

5. The D/A converter that is part of the composite A/D converter showed a malfunction. For a given digital input, the voltage out of the D/A converter changed discontinuously by an amount corresponding to over 300 gamma at a

temperature of slightly over 45°C. The exact temperature at which the change occurred varied during the course of the tests. Because of the use of auto-calibration or "chopper stabilization" for the complete converter, this change did not adversely affect the performance of the composite converter. However, because of this malfunction, some of the tests were not performed above 45°C.

6. A small scale nonlinearity was observed in the composite A/D converter. A linearity curve was made by plotting the converter digital output against the magnetic field input, and a deviation from linearity curve was made by subtracting the best straight line from the linearity curve. The deviation from linearity curve showed a roughly sinusoidal variation of ± 2 gamma amplitude and 64 gamma period. Sixty four gamma corresponds to one digital window of the component A/D converter. This nonlinearity is apparently a second order effect. If the component A/D converter were perfectly linear, the 256 readings of the component A/D converter that correspond to one cycle of the composite A/D converter would be evenly distributed (with proper adjustment) throughout the digital window of the converter, and no nonlinearity would result for the composite converter. A means for eliminating this nonlinearity has been devised and is discussed in the following section. The necessary changes to the converter were too extensive to make during the time period covered by this report.

7. A crosstalk test was performed on the converter. The reference zener diode was disconnected and a sinusoidal voltage of amplitude corresponding to ± 64000 gamma and .001 Hz frequency was applied to the converter in place of the reference voltage. The magnetometer was also disconnected and reference ground was applied to the converter in its place. Thus Channel 1 of the converter was connected to the ± 64000 gamma sinusoid while Channels 2 and 3 were connected to reference ground. The difference in the digital readings for Channels 2 and 3

were converted to gamma. This difference varied from +0.32 gamma to -0.32 gamma. The mechanism for the production of this crosstalk was not isolated. This amount of crosstalk is small in comparison to the amount expected due to sensor interaction.

In the following tables, results of some temperature tests are given. The first three columns in the tables are the digital outputs for channels 1, 2, and 3 of the composite converter. Input for channel 1 is the reference voltage, for channel 2 the input is reference ground, while for channel 3, the input is the magnetometer output. Column 4 in the tables is the difference between column 1 and column 2, while column 5 is the difference between column 3 and column 2, divided by column 4, and multiplied by a scale factor to convert the reading to gammas. Column 5 is thus the magnetometer output expressed in gammas. Each of the readings is the average of 256 readings from the composite converter, and each reading of the composite converter is the average of 256 readings of the component A/D converter. Thus, each reading shown is the average of 65, 536 readings of the component A/D converter. Units for the first four columns are one digital window of the component A/D converter, which corresponds to 64 gammas, approximately. The first table (table 1) is a zero offset temperature test run on Feb. 25, 1977. All four breadboards and the interface box were placed in a temperature test chamber for this test. The sensor, power supply, and minicomputer were not inside the temperature test chamber. The sensor was inside a mu-metal shield.

Table 1

Zero Offset Temperature Test

TEMP.	CH.1	CH.2	CH.3	Δ	FIELD
30°C	2776.266	2054.355	2054.376	721.911	1.33
15°C	2776.323	2054.390	2054.420	721.932	1.85
55°C	2781.344	2060.246	2060.299	721.099	3.31
35°C	2776.095	2054.153	2054.186	721.943	2.06
45°C	2775.983	2054.032	2054.056	721.951	1.49
50°C	2775.906	2053.931	2053.960	721.976	1.84
-5°C	2776.639	2054.651	2054.682	721.989	1.92
-25°C	2776.956	2054.938	2054.957	722.019	1.20
15°C	2776.356	2054.432	2054.469	721.924	2.30
25°C	2776.161	2054.224	2054.245	721.937	1.34

The next table (table 2) is a zero offset temperature test for the converter portion of the magnetometer only. It was run on March 1, 1977. The magnetometer output was disconnected from the converter input (ch 3) and channel 3 was connected to reference ground, the same as channel 2. The converter and interface box were inside the temperature test chamber.

Table 2

Zero Offset Temperature Test - Converter Only

TEMP.	CH.1	CH.2	CH.3	Δ	FIELD
15°C	2776.281	2054.340	2054.353	721.941	0.82
55°C	2781.264	2060.124	2060.171	721.140	2.91
45°C	2775.932	2053.964	2054.001	721.969	2.32
-25°C	2776.896	2054.860	2054.880	722.036	1.24
15°C	2776.291	2054.352	2054.365	721.940	0.87

Note the anomalous readings for channels 1, 2, and 3 at 55°C for both temperature tests. The source of these anomalous readings was isolated to a malfunction in the D/A converter as discussed earlier. Since one unit for these three channels corresponds to 64 gammas, the discontinuity corresponds to over 300 gamma. However, due to the use of autocalibration (or "chopper stabilization"), the final output, FIELD, only changes by about one gamma from 45°C to 55°C.

The offset variation from -25°C to +45°C just about meets the stated goals for the Magsat magnetometer, although it is considerably larger than the calculated values given in the interim report. Most of the offset variation appears to be due to the converter. It would be considerably larger if autocalibration were not used. The writer believes that a major portion of this offset variation is due to the same cause as the small scale nonlinearity discussed earlier, and that the offset variation would be considerably reduced by the changes recommended in the following section.

The next table (table 3) is a full scale temperature test for the entire magnetometer. The op amps used in the converter had been changed from Burr Brown 3550 K to Burr Brown 3506 J since the preceding tests were run. The entire magnetometer except for the sensor, power supply, and mini-computer were placed in a temperature test chamber. The sensor was placed inside a mu-metal shield, and a field applied to the sensor by means of a coil arrangement and a regulated power supply. The test was run on March 19, 1977.

Table 3

Full Scale Temperature Test

TEMP	CH.1	CH.2	CH.3	Δ	FIELD
-25°C	2778.748	2056.106	3029.612	722.642	60352.21
-5°C	2778.553	2055.861	3029.455	722.692	60353.48
15°C	2778.344	2055.676	3029.226	722.668	60352.82
35°C	2783.429	2061.600	3033.882	721.829	60344.24
55°C	2783.158	2061.233	3033.512	721.924	60336.06
75°C	2782.988	2060.968	3033.212	722.020	60325.92
15°C	2783.542	2061.702	3033.878	721.839	60336.77
-5°C	2778.504	2055.808	3029.160	722.696	60338.15

The malfunction of the D/A converter occurred at a lower temperature than previously, and occurred at a lower temperature when the temperature was being lowered than when it was being increased. Because of the use of autocalibration, this malfunction did not cause a serious error. From the readings at -25°C and +75°C, one can compute an average temperature coefficient of 0.27 gamma/°C. This is about four times greater than calculated and slightly exceeds the goal for the Magsat mission. Since there was some hysteresis in the measurements, possibly due to drift of the field applied to the sensor, the above figure is conservative. If one uses the readings for 75°C and -5°C, he computes 0.15 gamma/°C, which is within the goal for the Magsat mission.

The next table (table 4) is a full-scale temperature test for the converter only. It was run on March 18, 1977, and Burr Brown 3506 J op amps

were used in the converter, the same as for the test of table 3.

Table 4

Full Scale Temperature Test - Converter Only

TEMP.	CH.1	CH.2	CH.3	Δ	FIELD
-25°C	2778.660	2055.926	3031.505	722.674	60478.05
-5°C	2778.413	2055.692	3031.316	722.721	60476.93
15°C	2778.237	2055.551	3031.167	722.686	60479.36
35°C	2778.030	2055.298	3030.952	722.732	60477.89
45°C	2777.923	2055.097	3030.848	722.825	60476.07
55°C	2783.123	2061.202	3035.773	721.921	60478.62
75°C	2783.018	2060.921	3035.661	722.096	60474.38
-45°C	2778.472	2055.767	3031.393	722.705	60478.44

Comparing table 3 and table 4, it is apparent that much of the temperature sensitivity for full scale signals is due to the analog portion of the magnetometer. This temperature sensitivity is greater than can be attributed to the Vishay Corporation feedback resistor used in the analog magnetometer. The precise source of this temperature sensitivity has not been isolated; possibly it may be due to variations in the shunt resistance of capacitors used in the filter preceding the feedback winding of the sensor.

The next table (table 5) is a full scale temperature test for the converter only, the same as table 4. The data were taken on March 2, 1977 before the op amps in the converter were changed to Burr Brown type 3506 J to reduce a nonlinearity. Burr Brown type 3550 K op amps were used.

Table 5

Full Scale Temperature Test - Converter Only

(Data taken before linearity was improved-see text)

TEMP.	CH.1	CH.2	CH.3	Δ	FIELD
45°C	2776.049	2054.003	2976.079	722.046	57211.00
-25°C	2777.024	2054.874	2977.273	722.149	57222.85
45°C	2775.967	2053.920	2975.977	722.047	57209.79

Comparing table 5 with table 4, it is apparent that the data of table 4 show much less temperature sensitivity. This is due to the change of op amps made to improve linearity.

A noise test was run on the magnetometer on Feb. 22, 1977. One hundred and eight readings were obtained for channels 1, 2, and 3 at a rate of three readings per channel per second. The rate was limited by the computer print-out capability, not the magnetometer. There was one reading per channel for each cycle of the composite converter, thus each reading was an average of 256 outputs from the component A/D converter. The RMS variation in the readings for each of the channels corresponded to 1.1 gamma, thus the RMS variation in the computed field value would be about 1.5 gamma. The distribution of the readings appeared to be Gaussian. The RMS variation could of course be reduced by averaging a number of readings together. This noise level is greater than estimated in the interim report. The writer believes that it might be reduced by the changes recommended in the following section.

Recommendation for Further Work:

Although the magnetometer tested appears to be a suitable magnetometer for the Magsat mission, it did not meet the goals for this mission in all respects, nor did it match the calculated and estimated performance parameters given in the interim report. In this section an improvement in design is outlined that the writer believes will accomplish the following objectives:

a) Greatly reduce the small scale nonlinearity described in the previous section.

b) Reduce instrument noise.

c) Reduce temperature sensitivity of the converter.

A system diagram for the instrument is shown in figure 1, and the behavior of the instrument is described in the interim report. The A/D converter shown on the diagram is a successive approximation type. Two important features may be noted on the diagram:

a) Autocalibration (or "chopper stabilization"). This is accomplished by including a reference voltage and reference

ground as inputs to the multiplexer. This feature, real
time autocalibration, is described by Hewlett-Packard Corp.
as being perhaps of greatest significance to most users of
their Model 3455 A digital voltmeter (reference 2).

b) A D/A converter and adder used to produce a composite
converter more linear than the component A/D converter. A
description of how this is accomplished is given in
reference 1.

It is proposed here that a cyclic A/D converter be substituted for the
successive approximation A/D converter shown in Figure 1. This cyclic
converter is shown in block diagram form in figure 2. Its principle of
operation is similar to that of the cyclic converter used in the John Fluke
Manufacturing Co. Model 8500 A digital voltmeter described in reference 3.
The resulting converter would thus contain the best features of instruments
manufactured by two of the most respected producers of digital voltmeters,
and would, in addition, contain a feature designed to improve linearity.

Referring to figure 2, an analog input from a sample and hold amplifier
is applied through a multiplexer to a successive approximation A/D converter.
At the end of an A/D conversion, the digital output of the A/D converter sets
the digital input to a D/A converter by way of a storage register. The
difference between the D/A output and the analog input is amplified and
measured by the A/D converter through the multiplexer. The storage register
holds the D/A converter input constant while the A/D converter is making its
measurement. The two successive outputs of the A/D converter constitute the
output of the cyclic converter. As a specific example, suppose that the D/A
converter and A/D converter are 12 bit converters, and that only the eight
most significant bits of the D/A converter are used. The differential amplifier
should then have a gain of 128. The digital output would then be the sum of

a) the digital number formed by the eight most significant

bits of the first A/D reading followed by eleven zeros, and

b) the digital number formed by the twelve bits of the

second A/D reading. The cyclic converter in this example

would thus be a 19 bit converter.

Note that the most critical element of this cyclic converter is the

D/A converter, as it determines the accuracy of the eight most significant

bits. Because of the use of the storage register, the amount of "bit switching"

for the D/A converter is much less than for the A/D converter. For a constant

analog input, the bits of the D/A converter will not switch at all.

In addition to the design improvement to the magnetometer discussed

above, it is recommended that further tests (e.g. long term stability,

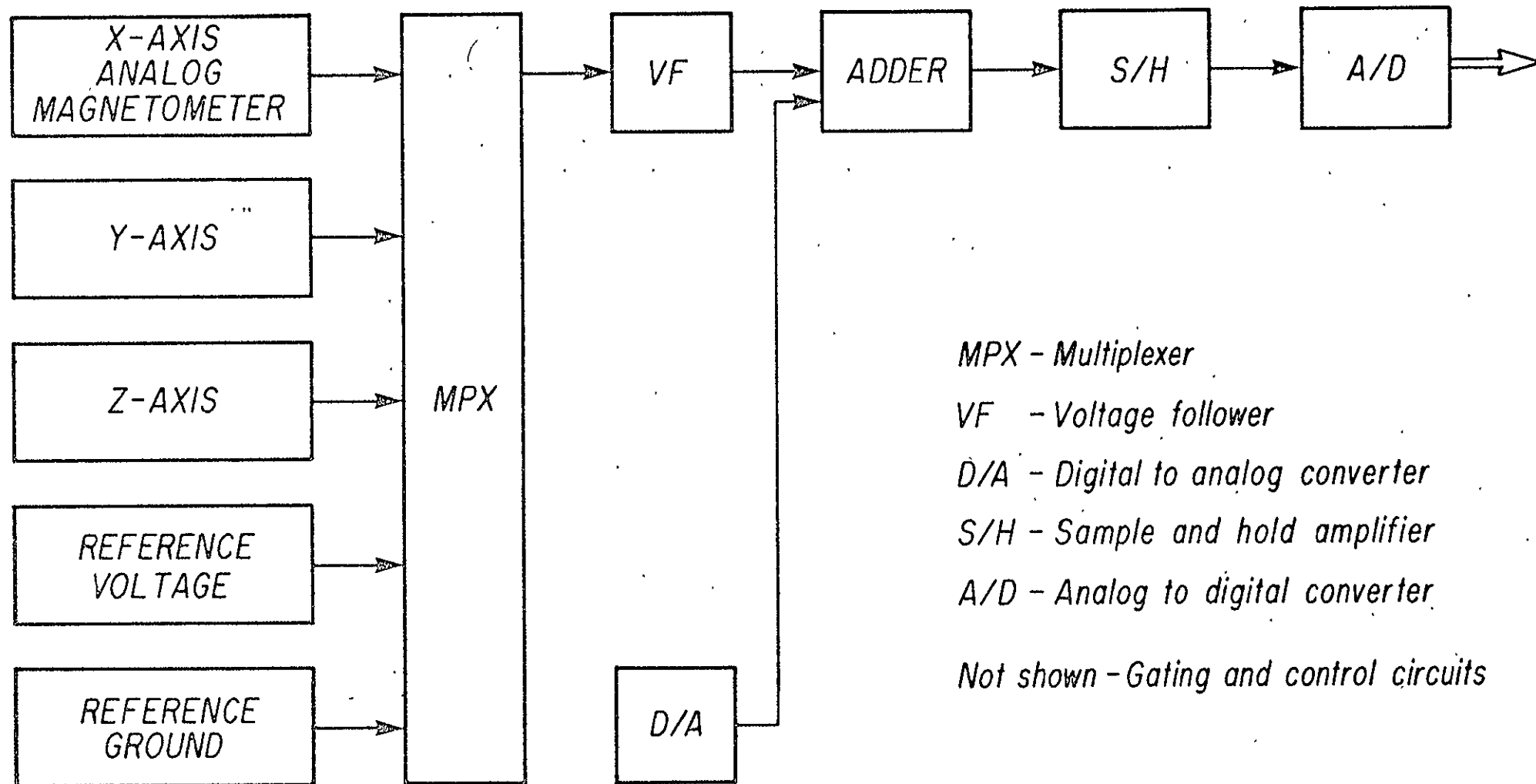linearity) be performed.

Conclusions:

The magnetometer tested performed well and appears to be suitable for the

Magsat mission, although not all the goals for this mission were met. The

improvement described in the body of this report is highly recommended. With

this improvement, the writer believes that the calculated performance para-

meters of the interim report (reference 1) would be met, and that the instrument

would be deserving of the appellation: "World's greatest triaxial digital
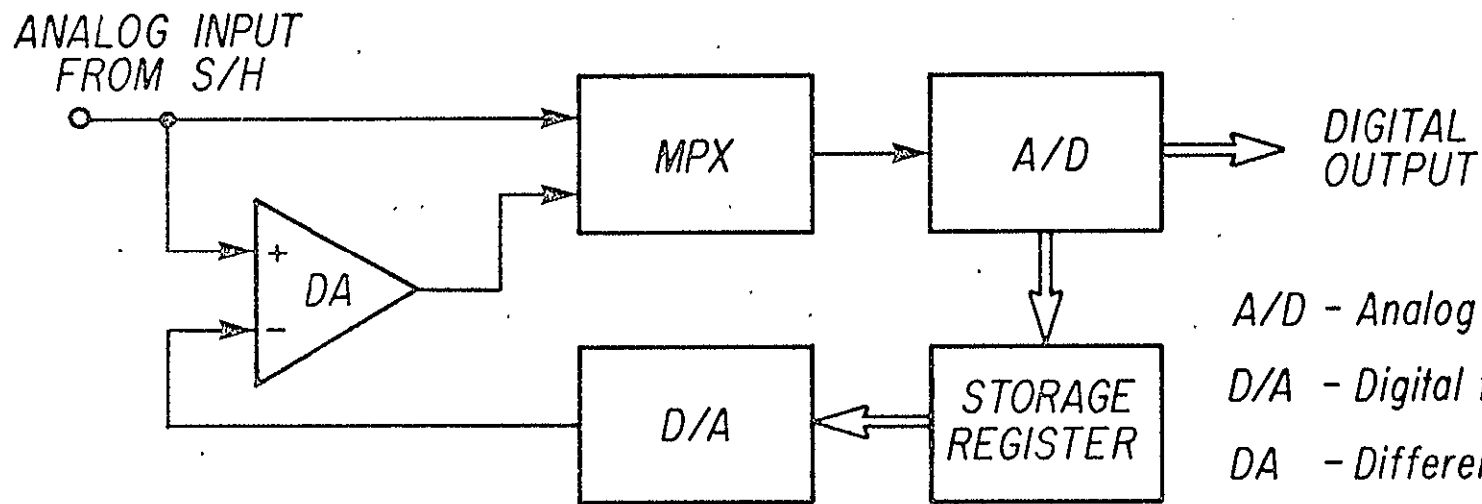
fluxgate magnetometer."

References:

McLeod, M.G., Interim Report on a Proposed Triaxial Digital Fluxgate Magnetometer
for NASA Applications Explorer Mission - A Design Study; Institute of Geophysics
and Planetary Physics Publication No. 1643, University of California, Los Angeles,
October 1976.

Gookin, A., A Fast-Reading, High Resolution Voltmeter that Calibrates Itself
Automatically; Hewlett Packard Journal, pp. 2-10, February 1977.

Koeman, R., and J. Reedholm, Error Correction Speeds Up a-d Conversion
Tenfold; Electronics, pp. 89-93, September 2, 1976.

X-AXIS ANALOG MAGNETOMETER			
Y-AXIS			
Z-AXIS	MPX	VF	ADDER → S/H → A/D →
REFERENCE VOLTAGE			
REFERENCE GROUND		D/A	

MPX – Multiplexer

VF – Voltage follower

D/A – Digital to analog converter

S/H – Sample and hold amplifier

A/D – Analog to digital converter

Not shown – Gating and control circuits

SYSTEM DIAGRAM-TRIAXIAL DIGITAL FLUXGATE MAGNETOMETER

14

Figure 2

ANALOG INPUT
FROM S/H

DIGITAL
OUTPUT

A/D – Analog to digital converter

D/A – Digital to analog converter

DA – Differential amplifier

MPX – Multiplexer switch

S/H – Sample and hold amplifier

Not shown – Gating and control circuits

CYCLIC ANALOG TO DIGITAL CONVERTER

Appendix A

Output Board

A schematic diagram of the output board is shown in figure 1A. Inputs 1 and 2 are connected to 100 K resistors in the demodulator, while outputs 1 and 2 are connected to the two ends of the sensor feedback winding. Outputs V_o and REF. GND. go to the multiplexer.

This is the same circuitry given in the interim report, except that:

a) The resistors connected to IN 1 and IN 2 (not shown, they are located on the second harmonic amplifier board) are 100 K instead of 1 M.

b) The ± 15 V supplies to the 490 chopper op amp are decoupled.

c) Capacitor C 19 was added to filter digital signals present on the reference ground and thus prevent these signals from ·interfering with the operation of the chopper op amp.

d) A more effective filter (C 16, C 20, C 21, R 3, R 15, R 17, R 18) was used between the sensor feedback winding and the chopper op amp. This filter reduces a signal present on the feedback winding at the fundamental frequency and its harmonics which interacts with the chopper amplifier and produces a signal at the second harmonic frequency. This signal at the second harmonic frequency is applied to the feedback winding and produces offset in the magnetometer output. This second harmonic signal is also reduced by the filter.

e) A resistor R 16 is added to increase the source impedance seen by the chopper op amp at the second harmonic frequency. This reduces the amount of second harmonic produced by the chopper op amp by the mechanism·described in (d) above.

Critical elements in this circuit are:

a) The feedback resistor R 10. This is a resistor manu-
factured by Vishay Corp.

b) Integrating capacitors C 1 and C 2. Shunt resistance
in these capacitors would reduce the ratio of open to closed
loop gain for the magnetometer. These capacitors are manu-
factured by Component Research Crop.

c) Capacitors C 11 and C 12. These capacitors shunt the
critical feedback resistor R 10, thus they should have high
shunt resistance. Units manufactured by Component Research
were used here.

d) Capacitors C 16 and C 20. Since they shunt the feedback
coil, they should have high shunt resistance. Polycarbonate
capacitors were used here, as sufficient time was not available
to obtain Component Research Corp. capacitors. Possibly the
capacitors used may have contributed to the temperature
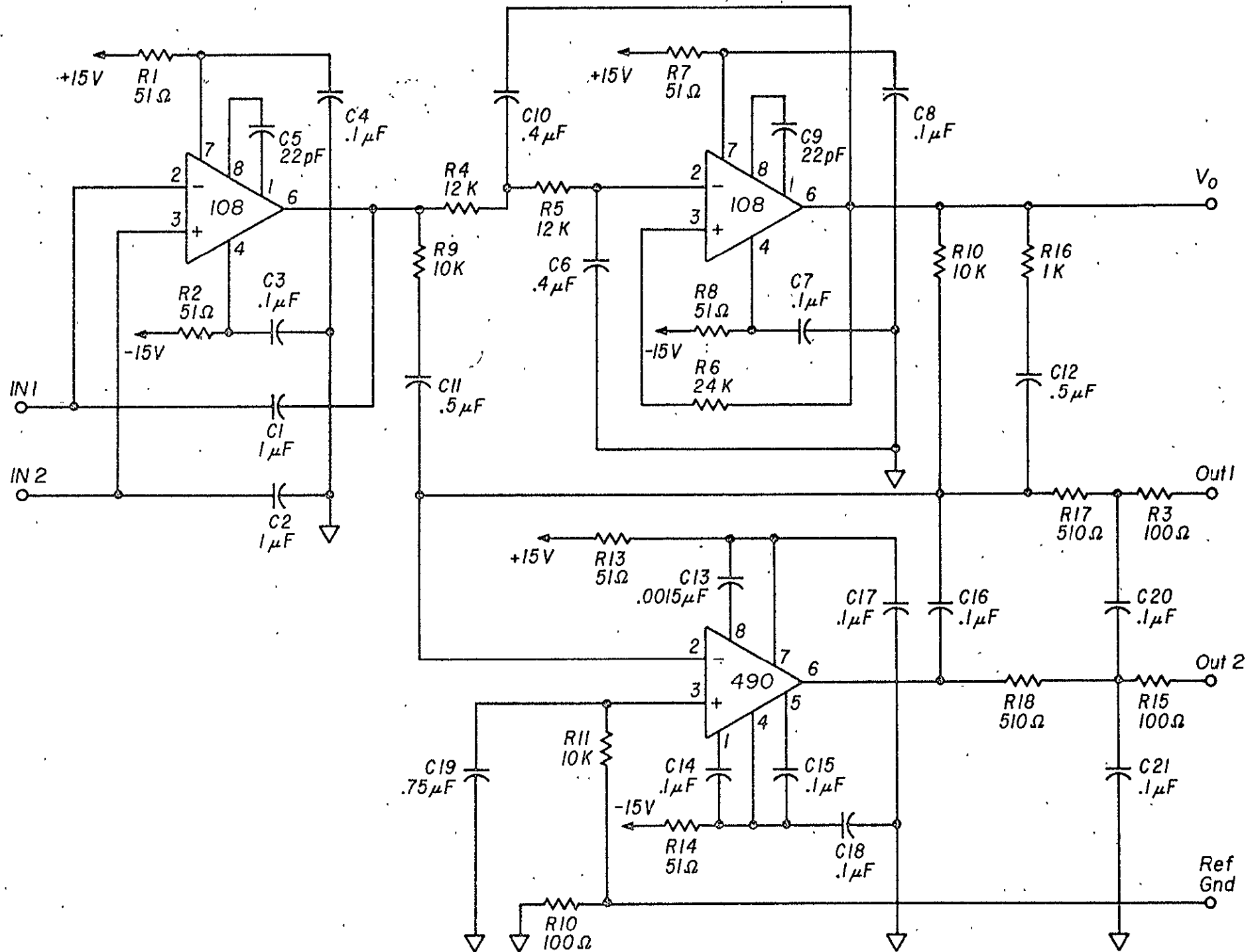sensitivity of the magnetometer.

Figure 1a

OUTPUT BOARD

18

Appendix B

Digital Board

A schematic diagram of the digital board is shown in figure 1B. It contains the analog to digital conversion portion of the magnetometer as well as the gating and control circuitry necessary to interface with the Hewlett Packard HP21MX minicomputer. This circuitry is the same as described in the interim report with the exceptions that:

a) Burr Brown type 3506 J op amps were used in the voltage follower and adder in place of Burr Brown type 3550 K. This change was made to improve linearity and temperature sensitivity.

b) A voltage output D/A converter was used instead of a current output converter, thus a separate op amp was not needed for use with the D/A converter.

c) Gating and control circuitry for interface with the minicomputer has been added.

Some of the components are not shown on this diagram, such as the resistors needed to convert the 4013 flip-flops to one shots, and the resistor and capacitor used to set the frequency of the 4047 multivibrator. Power supply and ground connections are not shown, neither are connections between different pins of the same component.

The unit has two analog inputs from the analog magnetometer, the magnetometer output Vo and reference ground. The other 5 analog inputs are not used.

Inputs from the computer are:

a) Device command (DC). This signal must be sent by the computer before the computer is able to read digital data.

b) Four bits of data divided into two parts: 3 bits (M)

elect the multiplexer channel and 1 bit (R) that serves as a

reset pulse.

Outputs to the computer are:

a) Device flag (DF). After the computer sends a signal to the digital board, a device flag signal must be received by the computer before it can send another signal. If the signal previously sent by the computer was a read data signal (DC), then the computer reads the data on receipt of the device flag (DF) signal.

b) 12 bits of digital data from the A/D converter.

A cycle of the conversion starts by the computer sending two identical commands to set the MPX using 3 data out bits. The reset pulse R is normally low, it goes high with the first command and low with the second. The reset pulse sets the down counter U 23 and U 24 to all 1's, sets the flip-flop U 21-2, and the first reset pulse causes a device flag pulse to be sent back to the computer. The second reset pulse causes the converter to convert and send a DF pulse to the computer at the end of the conversion. Thus the computer receives DF pulses with each of the two reset commands, which are required since the computer sends out DC pulses with each of these commands. These two DC pulses do not reset the U 21-2 flip flop, since the flip flop is being set at the same time by the reset pulses. This is mechanized by the use of one shots U 12-1, U 12-2, and U 21-1. The pulses from the first two one shots overlap the pulse from the third.

After a few milliseconds the computer sends a DC pulse which resets flip flop U 21-2 that starts the astable multivibrator U 25. This causes the S/H to hold and the A/D to convert, a status signal S from the A/D keeps the S/H in hold until the end of conversion or the negative portion of the multivibrator cycle, whichever comes later. At this time the one shot U 17-2

is triggered and it sends a DF pulse to the computer signalling it to read the A/D output. This is the first A/D output used by the computer. When the multivibrator signal goes negative, it steps the counter down one count. When the computer receives the DF pulse and after reading the A/D output, it immediately (within a few microseconds) sends a DC signal and is prepared to read the next A/D output. This will happen after the multivibrator goes positive to initiate another A/D conversion. After the computer has read 256 A/D outputs, the cycle is complete and the computer will send no more DC pulses. The MSB of the downcounter changes at this point, which sets the flip flop U 21-2 and stops the multivibrator. The down counter will be set to all 1's at this point.

Next the computer sends a reset pulse and switches the MPX to another channel. The computer switches the MPX to REF VOLTAGE, REF. GROUND, and MAGNETOMETER OUTPUT in succession, accumulates 256 readings from each channel, and then adds the 256 readings for each channel to produce a digital output for the channel.

Figure 1b
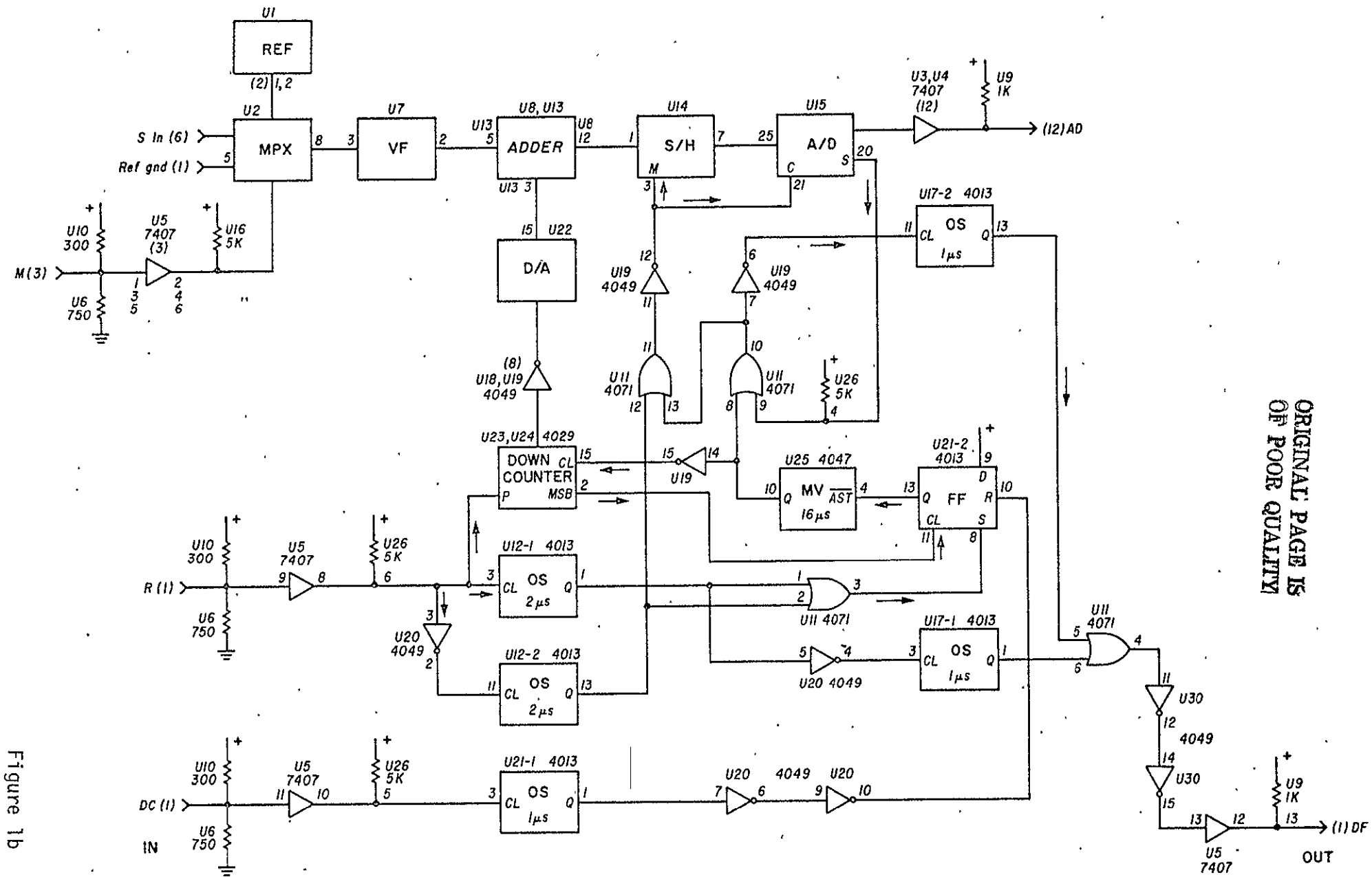
DIGITAL BOARD

Interim Report on a Proposed

Triaxial Digital Fluxgate Magnetometer

for NASA Applications Explorer Mission

A Design Study

M.G. McLeod

Acknowledgement

Numerous persons have made contributions to this design study. Particular note is made of the contributions of J.D. Means who suggested use of a microprocessor, supplied a major portion of the literature cited, and engaged in a number of valuable discussions with the writer.

The magnetometer described in this report is based in large measure on previous fluxgate magnetometers designed and developed at UCLA. Persons instrumental in the development and use of these magnetometers for space and ground-based measurements include: R.C. Snare, F.R. George, J.D. Means, J.J. Power, C.R. Benjamin, C.T. Russell, R.L. McPherron, and P.J. Coleman.

Table of Contents

List of Figures

A Proposed

Triaxial Digital Fluxgate Magnetometer for

NASA Applications Explorer Mission
A Design Study

1. Introduction:

This report describes a triaxial digital fluxgate magnetometer suitable for use on the NASA Applications Explorer Mission (AEM) spacecraft, which is known as Mag-Sat. The ultimate in performance is desirable for this mission.

In order to carry out this design study and make calculations of the relevant performance parameters, it was necessary to explore the limitations of presently existing space magnetometers and to consider how these might be modified to achieve the goals of the proposed mission. No presently existing space magnetometer was found capable of meeting these goals. It was found to be possible to make some modifications to previous magnetometers developed at UCLA for use on the ISEE and Pioneer Venus missions and achieve quite dramatic improvement in some of the basic performance parameters, particularly linearity and zero offset and changes in these parameters with time and temperature.

This report describes a triaxial digital fluxgate magnetometer believed to be capable of meeting the goals of the proposed mission, at least to the extent that the performance parameters are known from the study and analysis carried out thus far. Specifications of the performance parameters that the magnetometer could be expected to meet are given in section 3.8. These specifications are given in such a way as to show the effects that the various elements of the magnetometer have on overall instrument performance. They are a guide to expected performance and are not intended as specifications to a manufacturer.

It is worth mentioning that the specifications of many of the performance parameters are much better than required by the goals of the proposed mission.

2. Features of the Proposed System:

The basic system block diagram is shown in Figure 1. The magnetometer contains a number of features in order to achieve high accuracy and excellent performance. They are:

(1) Signals from three analog fluxgate magnetometers measuring magnetic field components along three orthogonal axes are applied to a multiplexer and then to an analog-to-digital converter. Analog ground and a reference voltage are also applied to the multiplexer. This feature allows gain and offset corrections to be made in the digital outputs by a microprocessor. The A/D converter is therefore "chopper stabilized," which reduces gain and offset variations and low frequency noise. Thus a highly stable A/D converter is not required.

(2) A novel A/D converter is used which provides high linearity and resolution (19 bits). This converter is described in Appendix A.

(3) Offset errors and noise due to operational amplifiers are nearly eliminated.

(4) The system is nearly independent of all resistors and other passive components except for a single feedback resistor in each of the three analog fluxgates. These three resistors are ultra ultra precision resistors having very low time and temperature drifts.

(5) An ultra-ultra precision zener diode is used as a reference voltage. This precision diode has very low time and temperature drift.

(6) A digital filter is included. This is superior to analog filters, since the transfer function is independent of components and the corner frequency can easily be varied.

(7) Fluxgate sensors developed by NOL are used. These sensors have good linearity because a special effort has been made in the design of the feedback coils to produce a uniform feedback magnetic field.

(8) An electrostatic shield is incorporated in the sensor between primary and secondary windings to reduce noise and offset.

(9) Current to the sensor feedback coils is provided through a chopper stabilized amplifier. This procedure nearly eliminates effects of coil resistance, contact resistance in connectors, resistance of connecting cable, thermoelectric e.m.f.'s in feedback path.

(10) The analog magnetometers and analog-to-digital conversion are functionally separate. This has advantages in development, manufacture, and testing.

(11) A maximum slew rate of 100,000 gamma/sec is achieved. It could be increased by a factor of nearly 100, if necessary, with some decrease in magnetometer zero offset stability.

3. System Description (including calculations)

3.1 Overall System

The overall system block diagram shown in Figure 1 is the same as for previous magnetometers developed at UCLA for use on the ISEE and Pioneer Venus missions, with the exception that analog ground and a reference voltage are supplied as signal inputs to the multiplexer in addition to signals from the three analog fluxgates. The elements of the block diagram, however, are not the same. While maximum use has been made of previous designs, a number of improvements and changes have been incorporated to improve performance to the level required for this mission. The analog-to-digital converter shown is a composite featuring high linearity and resolution. The gating and control circuitry (as proposed, but not yet designed), includes a microprocessor which reduces the number of integrated circuit

chips required and permits more data processing to be performed on the spacecraft. Improvements have also been incorporated in the analog fluxgate magnetometers.

Referring to Figure 1, signals from the three analog fluxgates together with a reference voltage and ground are applied to a multiplexer. The multiplexer samples the three fluxgate signals in succession, then analog ground, the three fluxgate signals again, and finally the reference voltage. The three fluxgates are sampled at a 50 Hz rate, the other two voltages at a 25 Hz rate. Time duration of each sample is 5 milliseconds. Each of the fluxgates contains a two section low pass filter with corner frequency at 25 Hz to reduce aliasing.

The detailed method of data processing by the microprocessor can easily be modified to optimize performance as determined by experimental methods. The simplest procedure is to subtract the digital reading correspond-ing to the most recent measurement of analog ground from each of the three digital readings corresponding to the measurement of the three components of magnetic field and from the most recent measurement of the reference voltage. Next, offset corrections are individually made to each of the three field readings. The three zero-corrected field readings can then be divided by the zero-corrected reference voltage reading and multiplied by three indivi-dual scale factors that convert the readings to convenient units and take into account the slightly different sensitivities of the three analog fluxgates. This procedure will result in measurement of each of the three field components, corrected for zero and gain drifts in the analog-to-digital converter, at a 50 Hz rate. The microprocessor can also be used to digitally filter these readings and supply digital samples of the three

field components at a slower rate. A slight modification of the above procedure would be to use digitally filtered versions of the ground and reference voltages in the computations to correct for zero and gain drifts. It is also possible to transmit digital signals corresponding to the five measured quantities and do the data processing in a ground based computer. It would. thus be possible to eliminate the microprocessor, however, more integrated circuit chips would be required, more telemetry capacity would be required, and testing of the instrument would be less convenient. As previously mentioned, the gating and control circuits have not yet been designed. Though their influence on the quality of the instrument performance is minimal, a considerable effort is required for the detailed design of these circuits. It is possible that a microprocessor capable of carrying out the computations indicated above at a 50 Hz rate may not be available.

3.2 Sensors

The sensors proposed are of the type produced by Naval Ordnance Laboratories (NOL) for use in the ISEE and Pioneer Venus magnetometers but with an electrostatic shield added to shield the sense winding from the drive winding. Similar sensors are shown in the article by Gordon and Brown (1972).

The sensors are of the ring core type. Sensitivity of the sensors is mainly determined by the feedback coil, it is 1 ma = 64,000 gamma. The feedback winding for these sensors has been especially designed to produce a nearly uniform feedback field, this results in good linearity as discussed in Appendix B and also lessens dependence of sensitivity on temperature. According to some tests conducted at UCLA, addition of an electrostatic

. shield is expected to result in reduced noise, drift, and offset compared to figures given below for the ISEE and Pioneer Venus sensors.

From data given in the article by Gordon and Brown (1972), the offset temperature coefficient has a maximum value over the range -40°C to +70°C of about .003 gamma/°C. The short term offset stability is very good, the offset changes less than $\pm$ .05 gamma in 24 hours. Data on the long term stability (weeks, months, or years) of offset, sensitivity, and magnetic axis direction, or effects of temperature on sensitivity and magnetic axis direction is not presently available.

Noise and offset for these sensors has been measured at UCLA, typical values are:

(a) offset: .7 gamma

(b) noise: 1) white noise component: 10^{-4} gamma^2/Hz to beyond 25 Hz

2) 1/f noise component: 10 milligamma rms/decade

The two noise components are equal at about 0.5 Hz, below this frequency the 1/f component dominates.

3.3 Analog Fluxgate Magnetometer

Figure 2 shows a system block diagram of a triaxial analog fluxgate magnetometer (the portion of the system preceding the multiplexer). Components for a single axis are shown. Portions of the sensor drive circuit are common to all three axes. Magnetometer sensitivity is 10v = 64,000 gamma.

The sensor is a ring core type fluxgate with drive, sense and feedback windings. The drive winding is driven with a signal D_X of frequency f_0 = 7.25 KHz. The sense winding output is a signal at frequency $2f_0$ = 14.5 KHz of amplitude proportional to the magnetic field component at the ring core in the direction of the magnetic axis. This field component is equal to the difference between the ambient field component in the magnetic axis direction

and a feedback field component proportional to the current I_{FBX} in the feedback winding. The sense winding output is amplified and filtered by a passband amplifier, then demodulated and integrated to produce a signal V_{SX}. This signal V_{SX} is next applied to a combination low pass filter and V/I converter which has two outputs, a current I_{FBX} proportional to V_{SX} and a voltage V_X which is a filtered version of V_{SX}. Expressing the above relations mathematically, we have:

(1) $\quad E_1 = A (B_X - H V_{SX})$

(2) $\quad V_{SX} = \dfrac{1}{sT_1} E_1$

where E_1 is the voltage into the integrator, s is the Laplace transform variable, and A, H, T_1 are constants (independent of frequency). The above equations are an idealization that assume an ideal integrator, neglect the effects of the passband filter which would make A frequency dependent, and treat the components of ambient field and feedback field in the magnetic axis direction as independent of the spatial variables. Eliminating E_1 from equations (1) and (2), we have:

(3) $\quad V_{SX} = \dfrac{B_X}{H} \dfrac{1}{1 + sT}$

where $T = T_1/(AH)$. Note that the DC value of the transfer function depends only on H, the feedback transfer function. It is independent of the forward transfer function, $A/(sT_1)$. This is a consequence of the use of an (ideal) integrator in the forward path. The time constant T depends on the integrator time constant T_1 and also on A and H.

We can take account of the passband filters and nonideal integrator by replacing equations (1) and (2) by:

(4) $\quad E_1 = A_0 F(s) [B_X - H V_{SX}]$

(5) $\quad V_{SX} = \dfrac{1}{sT_1} \dfrac{sT_2}{1 + sT_2} E_1$

where F(s) is a transfer function dependent on the passband filters transfer function while the added term in (5) takes account of the fact that the integrator gain is finite at DC. The main effect of F(s) is to introduce phase shift, and we can approximate it by:

$$(6) \quad F(s) = \frac{1 - sT_3}{1 + sT_3}$$

Using the expression (6) for F(s) and eliminating E_1 from (4) and (5), we find approximately:

$$(7) \quad V_{SX} = \frac{1}{H \left(1 + \frac{T}{T_2}\right)} \frac{1 + sT_3}{1 + s(T-T_3) + s^2 T\, T_3} F(s)\, B_X$$

where we have made the assumption that:

$$(8) \quad T_2 \gg T$$

and $T \doteq T_1/(A_0 H)$. T/T_2 is the ratio of closed loop to open loop gain for the magnetometer and should be made as small as possible for best gain stability. It is shown in section 3.3.3 that this ratio is about 10^{-8}. Note that the magnetometer will oscillate for $T < T_3$.

The transfer function in (7) (neglecting F(s)) is maximally flat if T is chosen so that:

$$(9) \quad T = 4 T_3$$

With this choice of T, which should give adequate margin of safety against oscillation, the three decibel point is given by:

$$(10) \quad f = \frac{1}{2\pi T_3} \left[\frac{1 + \sqrt{65}}{32}\right]^{1/2} = .0847/T_3$$

For the passband filters used, T_3 is approximately $.25 \times 10^{-3}$ seconds, so the corner frequency given by (10) is 340 Hz.

The offset voltage (unnulled) associated with the integrator is less than one millivolt. If we arbitrarily decide to make this offset correspond to one percent of the offset field associated with the sensor, we must choose $A_0 = 1.0$ mv/.007 gamma. For a sensitivity of 10 V equal to 64,000 gamma, we must have

H = 6400 gamma/volt. For a maximally flat response, T = 1 millisecond. Then from the definition $T = T_1/(A_0H)$, we find T_1 = 0.9 seconds. We must choose this integrator time constant to have a value of 0.9 seconds or larger if we wish the offset associated with the integrator to be less than one percent of the offset associated with the sensor. Now there is a maximum voltage for E_1, the integrator input, which is on the order of 14V. This means that the maximum rate of change for V_{SX} is 14V/0.9 seconds, or in terms of magnetic field, 100,000 gamma/second. We see that the magnetometer is slew rate limited due to use of an integrator in the forward path. If we wished to reduce the offset field associated with the integrator below one percent of the sensor offset field, we would have to further limit the slew rate or use an op amp with less offset voltage in the integrator.

The lowpass filters preceding the magnetometer output have the transfer function:

$$(11) \quad V_X = \frac{1}{(1 + s \cdot T_L)^2} V_{SX}$$

where T_L is the time constant associated with the lowpass filters. To reduce aliasing when the output is sampled at a 50 Hz rate, T_L is chosen so that $1/(2\pi T_L)$ = 25 Hz. Combining (11) and (7), and noting that the time constant associated with (7) is much smaller than that associated with (11), we have approximately:

$$(12) \quad V_X = \frac{1}{H} \cdot \frac{1}{(1 + s \, T_L)^2} B_X$$

The electronic circuits making up the elements shown in Figure 2 are basically the same as those given in the report by Power (1973), however, a number of changes have been made to improve performance. The greatest changes are in the elements labeled "L.P. Filter and V/I Converter" and "Sensor Drive Circuit." All of the electronic circuits are discussed in the following subsections of this report.

3.3.1 Sensor Drive Circuit

The purpose of the sensor drive circuit is to produce three sine wave voltages having very low second harmonic distortion for driving each of the three sensors through a series resistor. The sensor drive winding represents a nonlinear impedance to the drive voltage. Voltage and current waveforms (idealized are shown in Figure 7 and are derived as follows: Assume no external magnetic field. Current through the drive winding produces a field H within the ring core. When the core is not in the saturation region, dB/dH is very large and the impedance of the drive winding is much larger than the series resistor R (which includes the ohmic resistance of the winding as well as an external resistance). Thus the back e.m.f. produced by the drive winding is nearly equal to the drive voltage, and the current I is nearly zero. Thus we have approximately:

$$(13) \quad V = K \frac{dB}{dt}$$

where the proportionality constant K depends on the number of turns and area of the drive winding.

For an applied voltage

$$(14) \quad V = A \sin \omega t$$

and for a core saturation field B_{SAT}, we get from (13) and (14), by integration:

$$(15) \quad 2B_{SAT} = \frac{A}{K\omega} [1 - \cos \omega T_1]$$

where we have assumed that the current required for saturation is negligible so that the core leaves saturation at t = 0. T_1 is the time at which the core again enters saturation. We can make $\omega T_1 = \pi/2$ by properly choosing the amplitude A of the drive voltage to satisfy (15). For the NOL sensors proposed, this requires a drive voltage of about 10 V peak-to-peak. When the core is in saturation, the current is determined by the series resistor R and the drive voltage. For

a 100 ma peak drive current, R (including sensor resistance) should then be 50 ohms. Exact values of the drive voltage and series resistor will vary somewhat from one sensor to another.

Operation of the flux gate for these waveforms is as described by Scouten (1972). For no external field, there is no net flux through the sense winding for either portion of the cycle (saturation or non-saturation), since the fluxes due to each half of the core are equal and opposite. If an external field component along the magnetic axis is present, there will be a net flux through the sense winding during each portion of the cycle, but the magnitude of the flux will be different for the saturation portion than for the non-saturation portion. The flux waveform will thus be a square wave at frequency $2f_0$ = 14.5 KHz and of amplitude proportional to the field component along the magnetic axis. The voltage detected at the sense winding would ideally then be proportional to the derivative of a square wave, however, due to capacitance across the winding, the higher frequencies are attenuated. Moreover, due to departures from the ideal, the fundamental frequency f_0 = 7.25 KHz and its harmonics are also present.

The sensor drive circuit is shown in Figure 3. A 29 KHz signal from the gating and control circuits is applied to a dual flip-flop to produce an output signal at frequency f_0 = 7.25 KHz. This signal is applied to a pair of transistors to produce a low output impedance square wave, 15 V peak-to-peak. Signals from the flip-flops are also sent through buffer amplifiers to produce a $2f_0$ = 14.5 KHz square wave used in the demodulator and an f_0 = 7.25 HKz square wave used for synchronization purposes in testing the instrument. The square wave output from the transistor pair is filtered to produce a nearly pure sine wave output. Tests at UCLA have shown that this sine wave has low second harmonic distortion for which the relative amplitude is only 15 parts per million of the fundamental, due primarily to

nonlinearities in the inductors that are elements of the filter. The sine wave output from the filter is used as an input signal to three drive amplifiers, one for the sensor associated with each axis. The drive amplifiers must be capable of supplying the current and voltage waveforms shown in Figure 7 to the sensor drive windings and should not introduce additional harmonic distortion to the sine wave. An op amp in conjunction with a pair of push-pull driver transistors supplies the required current and voltage to the sensor drive winding through a series resistor. Feedback from the push-pull output to the op amp input is used to minimize harmonic distortion. The feedback resistor is selected to obtain the current waveform shape shown in Figure 7 (50-50 duty cycle), while the resistor in series with the output is selected to obtain the desired peak current amplitude (100 ma). Approximate value for the feedback resistor is 50K, for the series resistor 50 ohms. An op amp with a high slew rate capability is used to minimize harmonic distortion.

Tests conducted at UCLA have shown that a second harmonic at the drive amplifier output of relative amplitude as low as 300 parts per million of the fundamental is sufficient to produce an offset at the magnetometer output corresponding to one gamma when using NOL sensors of the type proposed. (These sensors did not have an electrostatic shield, however.) It is, therefore, important to use considerable care in the physical arrangement of components to avoid coupling second harmonic signal present in other portions of the instrument into the drive circuit, either through capacity coupling or through the power supply. A large amount of second harmonic signal (tens of milliamperes) flows in each collector of the drive transistors because of the push-pull arrangement, thus filtering is required to prevent this second harmonic signal from flowing into the power supply or circuit

ground. The components attached to the op amp inputs should be physically

located as close as possible to these inputs to minimize the capacity to other

portions of the circuit. It has been found in tests conducted at UCLA that,

if these precautions are taken, no measurable second harmonic distortion

is introduced by the drive circuit beyond the 15 parts per million due to

nonlinearities in the passive filter. If these precautions are not taken,

second harmonic distortion may easily be two orders of magnitude greater and

produce offsets of 5 gamma or more. For the circuit shown and with the

precautions indicated, maximum offset introduced is 0.05 gamma.

3.3.2 Second Harmonic Amplifier

The second harmonic passband amplifier is shown in Figure 4 and is identical

to second harmonic amplifiers used with previous fluxgate magnetometers designed at

UCLA and described in the report by Power (1973), except that gain must be

adjusted to provide the proper value of magnetometer time constant T as discussed

in section 3.3 Analog Fluxgate Magnetometer. The input to this amplifier is the

signal present on the sense winding of the sensor, while the output is an

amplified version of the second harmonic component of this signal. Filters are

included to remove the undesired harmonics which would cause "clipping" if not

filtered out. It has been found empirically that the filters shown, each of

which has three pole pairs and a bandwidth of $\pm$ 7.5% of the 14.5 KHz center

frequency, are adequate for this purpose. Just as with the drive amplifiers

discussed in the previous section, it is important to avoid coupling second

harmonic signal present in other portions of the instrument into this circuit,

especially into the first stages. Thus components connected to the op amp

inputs should be located physically close to these inputs and the power

supply should be adequately filtered. Tests conducted at UCLA have shown

that the noise introduced by this amplifier and measured at the magnetometer output is less than 10% of the noise due to the sensor. This was determined by inserting an attenuator between the sensor and second harmonic amplifier and increasing the attenuation until the noise at the magnetometer output increased by a factor of $\sqrt{2}$.

3.3.3 Demodulator and Integrator

The first stage of this circuit is an all pass network used to adjust the phase of the input signal from the second harmonic amplifier so that at the output of the all pass network the second harmonic signal is either in phase or 180° out of phase with the square wave demodulator drive signal. (Whether or not there should be zero or 180° phase shift depends upon which direction the feedback current flows through the sensor feedback winding, and whethe $2f_0$ or $\overline{2f_0}$ is used as the demodulator drive.) Because of the use of feedback in the analog fluxgate and the presence of an integrator in the forward path, when the sensor is in a steady (non time-varying) magnetic field, any in phase second harmonic signal at the input to the demodulator is reduced nearly to zero. Thus any quadrature component that may be present due, for example, to second harmonic in the sensor drive signal, will dominate at the demodulator input. It is convenient in adjusting the phase of the magnetic field dependent second harmonic at the demodulator input to apply a 60 Hz magnetic field to the sensor which will produce a second harmonic component amplitude modulated at 60 Hz at the demodulator input. The phase shift of the all pass network can then be adjusted so that the modulated second harmonic is either in phase or 180° out of phase with the square wave demodulator drive signal.

The transfer function for the all pass network is

$$(16) \quad H(s) = \frac{-1 + s\,T_A}{1 + s\,T_A}$$

where T_A is the RC time constant of the 2000 pF capacitor and the resistor

to be selected to adjust phase shift. As the resistor varies from zero

to infinity, the phase shift varies from + 180° to 0°. For a resistance of 5K,

the phase shift is approximately 90°.

Demodulation is accomplished by alternately switching an operational

amplifier from an inverting to a non-inverting mode using a double pole / double

throw Mosfet switch. The operational amplifier is connected as a differential

input integrator with time constant T_1 chosen to be one second in accordance

with the discussion in section 3.3 Analog Fluxgate Magnetometer.

The LM108A op amp has a maximum offset voltage of .5mv with a temperature

coefficient of 5 $\mu V/°C$ and a maximum offset current of 0.2 nA with a temperature

coefficient of 2.5 pA/°C. For the 1M source impedance used, this gives a maximum

total offset voltage (including that due to the offset current) of 0.7 mv with

a maximum temperature coefficient of 7.5 $\mu V/°C$. Drift with time is not specified,

a reasonable estimate based on figures for Analog Devices AD504J-op amp which

has similar characteristics would be 50 $\mu V/year$. For A_0 = 1mv/.007 gamma

as discussed in section 3.3 Analog Fluxgate Magnetometer, this means that the

integrator can produce a maximum offset of 0.005 gamma with a temperature

coefficient of .00005 gamma/°C and time drift of .0003 gamma/year.

Since the voltage gain of the LM108A is greater than 10^5, T_2 is greater than

T_1 by the same factor so T_2 is greater than 10^5 seconds, where T_1 and T_2 are

defined in section 3.3 Analog Fluxgate Magnetometer. Thus the ratio T/T_2

appearing in equation (7) is less than 10^{-8} and equation (8) is satisfied.

The ratio T/T_2 is also the ratio of closed loop to open loop gain for the

magnetometer. Note: To obtain the high ratio of T_2/T_1 indicated, capacitors

with high insulation resistance should be used. Component Research Co., Type

05TA105 is a 1μF Teflon capacitor with a shunt resistance greater than 10^5

megohms from 25°C to 85°C, decreasing at 125°C to 10^4 megohms, appears suitable, and is made to NASA quality control specifications.

The circuit shown here is identical to that shown in the report by Power (1973) except that one op amp preceding the integrator has been eliminated and the integrator time constant is different. The circuit given here produces less offset and introduces less second harmonic into the power supply.

3.3.4   Lowpass Filter and Voltage/Current Converter

The lowpass filter and voltage/current converter is shown in Figure 6. This circuit performs two functions: (a) It filters the analog magnetometer output in order to reduce aliasing when this output is the input to a sampled data system and provides a low output impedance to this system (b) It provides a feedback current, proportional to the input signal V_{SX}, to the feedback winding of the sensor.

The feedback current I_{FB} flows into a virtual ground produced by the op amp in the lower portion of the figure, i.e. the negative input terminal of this op amp may be treated as ground initially for the purpose of calculating I_{FB} and V_X. The circuit shown in the upper portion of the figure is a two pole low pass filter with transfer function given earlier in equation (11) which is repeated here:

$$(11) \quad V_X = \frac{1}{(1 + s\, T_L)^2}\, V_{SX}$$

This lowpass filter is identical to the one described in the report by Power (1973) except that different component values are used. The current I_{FB} is the sum of the two currents I_1 and I_2, where I_1 is the current flowing from V_{SX} through the series RC while I_2 is the current flowing from V_X through the parallel RC. We have, since $RC = T_L$:

$$(17) \quad I_1 = \frac{s\, T_L}{1 + s\, T_L}\, V_{SX}/R$$

(18) $I_2 = (1 + s\,T_L)\,V_X/R$

combining (11), (17), and (18), we get:

(19) $I_{FB} = V_{SX}/R$

The reason for this somewhat complex method of generating the feedback current I_{FB} is so that the op amp associated with the lowpass filter will be inside the magnetometer feedback loop for DC signals. Because of the large DC gain of the preceding integrator circuit, the offset voltage associated with the lowpass filter op amp will then produce negligible offset at the magnetometer output, as it will be a factor of 10^5 less than the offset due to the integrator. If the magnetometer feedback loop were closed before the lowpass filter, the offset error associated with the filter op amp could be as much as 0.5 mv which would correspond to 3.2 gamma and the temperature coefficient of the offset could be as much as .032 gamma/°C.

The feedback winding of the sensor is connected between the output and negative input terminal of a chopper stabilized op-amp, the current I_{FB} flows into the junction between the feedback winding and negative op amp input, and the positive input terminal of the op amp is connected to ground through substantially the same impedance as the source impedance from which I_{FB} flows. Because the input impedance to this op amp is typically 100 M and the feedback winding resistance about 100 ohms, while the op amp gain is over 10^8 at DC and over 10^6 at 25 Hz, the current through the feedback winding is substantially equal to I_{FB}, differing by only about one part in 10^{14} for DC (not including offset current). If an op amp were not used here, the feedback current would be dependent on the feedback winding resistance, resistance of the connecting cable, contact resistance in the connectors, thermal e.m.f.'s generated at the connectors, and changes in these quantities with temperature and time.

The use of an op amp eliminates these sources of error, however, the op amp introduces errors due to offset voltages and currents, changes in these quantities with time and temperature, and input voltage and current noise. A chopper stabilized op amp is used here because the use of a chopper minimizes the sources of error mentioned. The unit chosen is Datel's AM-490-2C which is the only monolithic chopper stabilized op amp that the writer has found. It is packaged in a TO-99 package, hermetically sealed, the same package used by many ordinary op amps. It has an offset voltage of 20 μV with a temperature coefficient of 0.1 $\mu V/°C$, an offset current of 50 pA with a temperature coefficient of 1 pA/°C. Voltage noise is less than 900 nV/$\sqrt{Hz}$ in the frequency range of interest (below 25 Hz) while current noise is 8 pA rms from .01 to 10 Hz. Offset voltage stability is 5 μV/year. For the 10K source resistance used, the offset current, current noise, and current temperature drift are negligible compared to the corresponding quantities associated with offset voltage. At the magnetometer output, these quantities produce an offset of 0.13 gamma with a temperature coefficient of .0006 gamma/°C and a drift of .03 gamma/year. The white noise is less than .36 x 10^{-4} gamma^2/Hz, about one-third the white noise power associated with the sensor. There is no 1/f noise component. If an ordinary op amp such as the LM108A used in the lowpass filter were used here, initial offset could be 3.2 gamma with a temperature coefficient as much as .03 gamma/°C and possible drift of 0.3 gamma/year.

Because currents of tens of milliamperes flow in the circuit ground for the magnetometer different points that are all supposedly at ground potential will be at   slightly different potentials. To provide a definite ground reference for the multiplexer, a ground reference is brought out from each of the three analog fluxgates, and these three references are all connected

to the ground input to the multiplexer. To understand the reason for
the 100 ohm resistor shown in Figure 6, consider the following.
Resistance of #18 wire is about .064 ohms/ft., a current of 10 ma through one foot
of this wire would create a potential difference of 0.64 mv. If we take
this as a possible potential difference between the analog grounds in the
different fluxgates, we see that the current through the reference output shown in
Figure 6 can not be greater than ten microamperes because of the 100 ohm resistor.
If the wire resistance between the reference analog ground output and the
multiplexer is .064 ohms corresponding to one foot of #18 wire, then the
reference ground at the chopper positive input might differ from the reference
ground at the multiplexer by .6 μV, producing an offset error in the
magnetometer output of .004 gamma. If the 100 ohm resistor were not used as
indicated, we might have 10 ma or more flowing in the connecting wire producing
an offset error of over 4 gamma, which could reasonably be expected to be
subject to fairly large time and temperature variations.

Because of the high ratio of open loop to closed loop gain of the magnetometer
for DC (about 10^8), the only component in the entire analog fluxgate magnetometer
apart from the sensor that has any significant influence on the magnetometer
sensitivity at very low frequencies is the resistor marked with an asterisk
in Figure 6. The resistor type selected for this critical application is the
best that the writer has found, an ultra precision hermetic sealed metal film
resistor from the HP202 series manufactured by Vishay Corp. These resistors
have temperature coefficients less than 1ppm / °C and drifts of less than 5 ppm/year.
For full scale signals of 64,000 gamma, this is .06 gamma/°C and 0.3 gamma/year.

The capacitor shown in parallel with the sensor feedback winding is to be
chosen to resonate with the feedback winding at 1500 Hz and thus filter higher
frequencies from the winding. The resistor in series with the winding is chosen
to provide critical damping for this filter.

No provision is made for trimming the precision feedback resistor or for providing an offset current to the chopper stabilized op amp for the purpose of adjusting the magnetometer gain or nulling the offset (primarily due to the sensor). It seems best to simply measure these quantities during calibration and correct for them in the microprocessor (or in the ground data processing if a microprocessor is not used).

Let us now consider what is accomplished by using a chopper stabilized op amp to supply the feedback current to the sensor as compared to the more obvious alternative of connecting the sensor between ground and the junction point for I_1 and I_2. Advantages of using the chopper stabilized op amp are:

(a) Effects of resistance of the cable to the sensor are eliminated, which means that the cable can be changed without affecting the calibration. Cable resistance of only one ohm would cause an error of 6.4 gamma for a full scale signal of 64,000 gamma. Similarly, problems with connector contact resistance are eliminated.

(b) Ground loop problems are avoided which could produce offsets of a few gamma as discussed earlier.

(c) Thermal e.m.f.'s at connectors which would be on the order of 10 $\mu V/°C$ are avoided, which would correspond to .06 gamma/°C and could be expected to be time varying. These e.m.f.'s should be compared to the 20 μV offset, .1 $\mu V/°C$ Tempco, and 5 $\mu V/yr$. drift for the op amp.

(d) Effects of feedback coil resistance temperature coefficient are eliminated. Coil resistance is about 100 ohms compared to the 10K feedback resistor. Since copper wire has a tempco of 40 ppm/°C, the tempco for the series combination of 10K plus 100 ohms would be 0.4 ppm/°C (temperature measured at the sensor) compared to the 1 ppm/°C (temperature at precision resistor) due to the precision resistor. 0.4 ppm/°C corresponds to .025 gamma/°C for a full scale signal of 64,000 gamma.

3.4 Reference Voltage

The voltage reference for the multiplexer is tentatively planned to be a National Semiconductor LM 199 temperature stabilized "buried" zener. This reference zener is described in an article by Dobkin (1976). To supply a reference voltage to the multiplexer, the LM 199 is connected as shown in Figure 8. Current through the zener is about 0.5 ma. Two connections are made from this circuit to the multiplexer, a reference voltage connection and an analog ground connection. It is important that the analog ground connection to the multiplexer be brought out from a point physically close to the anode of the zener in order to avoid introducing errors that could arise from current flow in the analog ground circuit of the magnetometer as discussed in section 3.3.4.

Temperature stability for the LM 199 is typically only 0.3 ppm/°C with long term stability of 5 to 20 ppm/1000 hours. Assuming a random walk type drift, this corresponds to 15 to 60 ppm/year, or 1 to -4-gamma/year for a full scale signal of 64,000 gamma. Long term stability is not impaired if the unit is switched on and off.

The ± 15 V supply for the magnetometer has not yet been chosen. If we assume a temperature coefficient for this supply of 0.05% / °C, it will change the temperature coefficient of the reference zener by only 0.02 ppm/°C, which is negligible compared to the 0.3 ppm/°C of the zener alone.

Noise for this zener is much less than for an ordinary zener because of the buried junction. Broad band noise (10 Hz to 10 KHz) is 7μV rms, which corresponds to 50×10^{-4} microvolts^2/Hz or 25×10^{-8} gamma^2/Hz for a full scale signal of 64,000 gamma. Peak-to-peak noise over 10 minutes from .01 to 10 Hz is 1.5μV, which is about 0.4 μV rms. If we assume this is 1/f noise, it corresponds to about 0.1μ V rms/decade or one milligamma rms/decade for a full scale signal of 64,000 gammas compared to ten milligamma rms/decade

for the sensor (without electrostatic shield).

Note: A number of firms, including National Semiconductor, Motorola, and Analog Devices currently offer, or are expected to offer, buried zener references. The choice of zener reference indicated above should be considered tentative, it is planned to pursue this topic further in hopes of obtaining improved long term stability compared to the value indicated above.

3.5 Multiplexer

The multiplexer proposed is the Siliconix Type DG508A. It is planned that the multiplexer will be followed by a Burr Brown Type 3550 K op amp voltage follower which is considered as part of the composite A/D converter. Bias current of the op amp (100 p A at 25°C) is much smaller than the maximum drain leakage of the multiplexer (20 nA at 25°C), both leakage currents double every 10°C. Flowing through the maximum 400 ohm multiplexer channel "on" resistance, the multiplexer drain leakage could cause an offset of 8 μV or .06 gamma at 25°C and 0.35 gamma at 50°C. Typical leakage current is over a factor of 30 smaller, therefore it is proposed to select a multiplexer with typical leakage or less. Maximum offset will then be .002 gamma at 25°C and 0.01 gamma at 50°C. Drift of leakage current with time is not specified. We can make an estimate by noting that National Semiconductor LH0042 FET op amp has typical leakage of 1 pA and drift of 0.1 pA/week. Assuming a random walk type drift, it seems reasonable to estimate that the leakage current for the multiplexer might drift by its initial value in the course of a year. Thus we estimate the offset drift for the multiplexer as 0.002 gamma/year. No noise figures are given for the multiplexer. Again, we can make an estimate by noting that the noise current for the LH0042 is less than 0.1 pA rms from 10 Hz to 10 KHz compared to leakage current of 1 pA. Using the same proportionality factor for the multiplexer, noise in

the band 10 Hz to 10 KHz would be 0.2 milligamma rms, which corresponds to 4×10^{-12} gamma^2/Hz. This compares to 10^{-4} gamma^2/Hz for the sensor, thus we conclude multiplexer noise is negligible.

3.6 Analog to Digital Converter (composite)

The composite analog-to-digital converter proposed is described in Appendix A. It achieves very high linearity and resolution (19 bits).

The elements proposed for the composite converter are Burr Brown model ADC85 analog-to-digital converter, Burr Brown model DAC 85 digital to analog converter, Burr Brown model 3550 K op amps, and Burr Brown model SHC85 sample and hold.

Because the composite analog to digital converter is effectively "chopper stabilized," it does not contribute to gain or offset errors of the complete digital magnetometer. Sufficient data is not available to reliably predict noise referred to the input. We can make a rough estimate by noting that Intech's A-856-16 analog to digital converter has about 25 microvolts rms noise referred to the input. If this converter were used in the composite converter which averages 256 individual measurements of the successive approximation converter, the rms noise for the composite converter would be $(25 \mu V/16) \times 2 = 3 \mu V$ rms (the factor of two arises because the summing amplifier in the composite converter has a gain of 1/2) spread over the frequency band 0-25 Hz. This is 0.36 microvolts^2/Hz or $.16 \times 10^{-4}$ gamma^2/Hz, about 1/6 of the white noise power associated with the sensor. This estimate could well be too low. Digitization noise for a 19 bit converter with 10 V full scale range is approximately $(10V/2\sqrt{3})/(2/10^6)$ or about 6 μV rms. This corresponds to about $.64 \times 10^{-4}$ gamma^2/Hz, a little less than the white noise power associated with the sensor.

The converter should not contribute to the 1/f noise spectrum of the magnetometer because of the use of "chopper stabilization."

3.7 Gating and Control

The gating and control circuits have not been designed. These circuits have very little influence on the performance specifications for the magnetometer. Nevertheless, a considerable design and development effort is required for the detailed design of these circuits, and their design is not contemplated under the present study contract.

3.8 Specifications

The performance parameters calculated and estimated in the previous sections are summarized in this section.

Noise, white, 0-25 Hz,   milligamma rms

(a)	Sensor (w/o shield)	50
(b)	Feedback chopper op amp	30
(c)	Multiplexer (est)	.01
(d)	A/D converter (est)	20
(e)	Digitization	40
(f)	Zener reference (full scale input)	2.5
(g)	Second harmonic amplifier	5
	TOTAL	75

Noise, 1/f,   milligamma rms/decade

(a)	Sensor (w/o shield)	10
(b)	Zener reference (full scale input)	1

Offset (initial, can be nulled to zero by microprocessor)   gamma (25°C)

(a)	Sensor (w/o shield)	0.7
(b)	Integrator	0.007

(c)	Drive circuit	0.05
(d)	Feedback chopper op amp	0.13
(e)	Multiplexer (selected)	0.002

Offset Temperature Coefficient,   milligamma/°C

(a)	Sensor (w/o shield)	3
(b)	Integrator	0.05
(c)	Feedback chopper op amp	0.6
(d)	Multiplexer (selected)(doubles every 10°C)	2 at 50°C

Sensitivity Temperature Coefficient   ppm/°C
  Note: 1 ppm/°C = .06 gamma/°C for full scale input

(a)	Sensor	unknown
(b)	Feedback resistor	1
(c)	Zener reference	0.3

Offset Drift with Time   milligamma/year

(a)	Sensor	unknown
(b)	Integrator	0.3
(c)	Feedback chopper op amp	30
(d)	Multiplexer (est)	2

Sensitivity Drift with Time   ppm/year
  Note: 1 ppm/year = .06 gamma/year for full scale input

(a)	Sensor	unknown
(b)	Feedback resistor	5
(c)	Zener reference (see discussion next section)	15

Nonlinearity (excluding sensor)(deviation from best straight line)

(a)	Initial value	$\pm$0.1 gamma
(b)	Drift with Time	0.1 gamma/year
(c)	Temperature coefficient	.001 gamma/°C

Sensor Nonlinearity   unknown

(Tests at UCLA have shown it to be better than $\pm$6 gamma,
 however, this is the limitation of the measurement,
 not the sensor)

Slew rate, maximum   (see discussion next section)   100,000 gamma/sec

Magnetic Axes Stability with Time and Temperature   unknown

3.9 Discussion

From a performance point of view, the magnetometer is described (for
DC and very low frequencies) by its sensitivity, zero offset, nonlinearity,
noise, and changes in these quantities with time and temperature. An attempt
has been made to keep the errors associated with each of these quantities
individually as small as seemed reasonably practical, even though, for
example, the possible error due to sensitivity drift with time is about
thirty times greater than the possible error due to zero offset drift with
time. Also, it has been considered worthwhile to make sensitivity changes
that affect the axes individually much smaller than the sensitivity changes
that occur simultaneously for all axes, such as the sensitivity changes due
to changes in the zener reference voltage with time. The reasons for the
above approach are:

. (a) When harmonic analysis (either in time or space) is performed on
the data, the different types of error produce different effects. Nonlin-
earities could be particularly bothersome, as they produce frequencies that
weren't present in the magnetic field.

(b) Schemes for in flight calibration, such as by the use of a scalar
magnetometer or by spinning the spacecraft, are simplified if some of the
types of errors mentioned are negligible, for example, if it can be assumed
that only sensitivity is unknown.

For the most part, the performance parameters specified in the previous
section meet or exceed all of the goals stated in the study contract.
However, at present we do not have data for all of the important parameters,
in particular, some of the parameters associated with the sensor. The white

noise is about 50% greater than the goal of 0.1 gamma zero-to-peak in a 25 Hz bandwidth. Possibly the white noise may be even greater, as the value listed for the A/D converter is only a rough estimate. Below about 0.1 Hz, the 1/f noise will dominate the white noise.

To obtain a sensitivity drift with time as low as that listed in the last section may require that the reference be selected. The question of best choice of zener reference is still being considered, other zener references that appear to have better stability are available but they are noisier.

To obtain the values listed for multiplexer offset, offset tempco, and offset drift requires that the multiplexer be selected to have leakage currents as low as those listed as typical by the manufacturer, since the maximum leakage currents are about 30 times greater than typical. Even without selection of the multiplexer, the magnetometer would still meet the goals listed in the study contract (not including the parameters not presently known).

· Because of the very small temperature coefficients associated with the sensitivity, offset, and linearity of the electronics portion of the magneto-meter (excluding sensor), no ovens are required for the electronics portion of the instrument to meet the design goals over the temperature range -10°C to +50°C.

The maximum slew rate for the magnetometer should be greater than the the maximum field derivative expected. The maximum slew rate listed could easily be increased at the expense of increased offset time and temperature drift due to the integrator, since both of these quantities are proportional to the maximum slew rate. The specifications of the previous section show that slew rate could be increased by a factor of nearly 100 before offset drift due to the integrator would be comparable to the offset drift for the entire instrument, which is itself very small. However, unless an increased slew rate is needed, there seems to be little point in introducing additional errors.

An additional source of offset error is thermoelectric effects at junctions
of dissimilar metals, such as junctions of the leads of circuit components
with the wiring of the printed circuit board. Typical thermocouple voltages
are about 10 µV/°C. Siliconix states that for their multiplexer in a
thermally stable environment, typical error developed across the switch is
3 µV, while in free air with room drafts it might be as much as 7 to 10 µV.
This would correspond to an offset error of about 0.1 gamma. This is perhaps
a reasonable estimate of how much the offset is likely to change in going
from the atmosphere to the vacuum of space, and illustrates the need for
minimizing thermal gradients in the environment.

Finally, since the use of a scalar magnetometer is being considered
for inflight calibration of the vector magnetometer, it should be mentioned
that the fluxgate magnetometer will cause the reading of the scalar
magnetometer to be in error as a measure of magnitude of the ambient field
that would be present in the absence of the fluxgate magnetometer. This is
true whether or not the fluxgate magnetometer is "on", "off", or partially
"on" (such as providing a drive signal but disconnecting the feedback coils).
The error can be expected to depend upon the distance between the two magneto-
meters and upon the angular orientation of the vector between the two instru-
ments in the coordinate system defined by the fluxgate magnetic axes. This
problem has not been considered in detail, however, some qualitative considera-
tions are noted here. Let us assume the fluxgate magnetometer is "on".
The total field vector at the scalar magnetometer is obtained by multiplying
the ambient field vector by a matrix. The elements of the matrix depend on
the location of the scalar magnetometer in the coordinate system defined
by the fluxgate axes. If a unit matrix is subtracted from this matrix, the
elements of the difference matrix can be expected in general to decrease with
increasing distance between the magnetometers as $1/r^3$, where r is the distance,

and r is assumed large relative to the dimensions of the fluxgate feedback windings. If one desires a field magnitude error of less than 1 ppm at the scalar magnetometer, one would expect, then, that the separation between the two magnetometers should be on the order of 100 times the dimensions of the feedback windings, or about 15 feet. Let us consider whether there is a best angular position for the scalar magnetometer in the fluxgate coordinate system. Symmetry considerations lead one to consider the following possibilities:

(a) A long one of the axes

(b) In the plane of two axes along the line bisecting the angle between the axes

(c) Along a line making equal angles with all three axes

For possibility (c), symmetry considerations lead us to conclude that the relation between the field vector at the scalar magnetometer and the field vector for the ambient field must be of the form:

$$
\begin{pmatrix} B_{XS} \\ B_{YS} \\ B_{ZS} \end{pmatrix} = \begin{pmatrix} a & b & b \\ b & a & b \\ b & b & a \end{pmatrix} \begin{pmatrix} B_X \\ B_Y \\ B_Z \end{pmatrix}
$$

This neglects the fact that sensors of finite dimensions cannot be arranged in such a way that their axes of symmetry intersect at a point halfway along each sensor. The field magnitude at the scalar magnetometer is related to the ambient field magnitude by

$$
\vec{B}_S \cdot \vec{B}_S = (a^2 + 2b^2)\, \vec{B} \cdot \vec{B} + 4\,ab\,(B_X B_Y + B_Y B_Z + B_Z B_X)
$$

Since cross terms are involved in the above equation, it is not possible to correct the scalar magnetometer reading to allow for the presence of the fluxgate by simply multiplying by a correction factor. Similar conclusions apply for possibilities (a) and (b) above.

By using the readings of the fluxgate magnetometer to correct the readings of the scalar magnetometer, it is possible to use much smaller magnetometer separations than indicated above. The ambient field magnitude can be determined from the equation:

$$B_A{}^2 = B_S{}^2 + a\, B_X{}^2 + b\, B_Y{}^2 + c\, B_Z{}^2 + d\, B_X B_Y + e\, B_Y B_Z + f\, B_Z B_X$$

where B_A is ambient field magnitude, B_S is scalar magnetometer reading, B_X, B_Y, B_Z are fluxgate magnetometer readings, and the coefficients a through f are parameters to be determined during calibration. In order that these parameters be small compared to unity, say on the order of 10^{-3}, the magneto-meter separation should be on the order of 1.5 feet or more. This subject deserves a more quantitative treatment.

4. Other Systems Considered

A number of other possible systems for producing a vector magnetometer were considered in addition to the system presented here.

The possibility of using a D/A converter in the feedback path of an analog fluxgate magnetometer to produce a "field offset" type magnetometer as discussed in Appendix B was considered but rejected in favor of the system presented here for the following reasons:

(a) If a hybrid converter of the bipolar type were used, such as the Burr Brown DAC85, both offset and gain stability would be limited by the stability of the resistor network in the D/A converter. This is 100 ppm/year, a much higher value than the offset stability of the system presented here.

(b) If the converter were used in a unipolar fashion by adding a DPDT switch, offset errors due to the resistor network would be eliminated, but offset errors due to switch leakage in the converter would be 1 ppm/°C, or about 0.1 gamma/°C. This is over thirty times greater than the value for the

system presented here. An oven would be required to meet the design goals of this mission.

(c) Slew rate would be severely limited.

(d) There is no apparent way to "chopper stabilize" the system.

(e) Linearity and linearity changes with time would be much worse than achieved with the present system, in fact, the design goals could not be met, unless a converter were built using more stable resistors.

(f) There are no apparent advantages to this system compared to the system presented here.

Another system considered was essentially the same as the one presented here, but using a tracking converter as an element of the composite converter. The tracking converter, in turn, would be built using a D/A converter. The advantage of a tracking converter is that it can make a conversion in a shorter time than a successive approximation converter, also accuracy should be better as there is less "bit switching" involved. However, a more complicated gating and control circuit would be required to lock the converter onto the signal following switching of the multiplexer from one channel to another. Development of such a converter would require considerably more time and funds than are available under the present study contract.

Use of a Helium magnetometer as a sensor was also considered. Data obtained from Al Frandsen at JPL indicate that noise levels of 10^{-5} gamma^2/Hz can be obtained, which is an order of magnitude (in power) better than the fluxgate sensor proposed here (without an electrostatic shield, we don't have figures for the improvement that a shield may produce). There is no 1/f noise (at least none has been measured), drift is 30 to 50 milligamma/year. We don't have figures for the drift of the fluxgate sensor, a reasonable

guess would be that the figures are comparable. The reason that the possible use of a Helium sensor has not been pursued further is the limited time and funds available under the present study contract and the fact that we are more familiar with fluxgate magnetometers. However, it should be noted that the problem of making a triaxial digital fluxgate magnetometer has much in common with the problem of making a triaxial digital Helium magnetometer. Both problems involve the accurate measurement of current through feedback coils and conversion of the measurement to a digital number. Thus, much of the system presented here would be applicable to the development of a triaxial digital Helium magnetometer.

Finally, the use of a triaxial coil system for the feedback coils, with all three sensors inside a single set of coils, has been considered. There is some reason to think that such a system may be better than the use of independent feedback windings for the three sensors, since all three components of the magnetic field at each sensor are nulled. Also, the magnetic axes for the magnetometer are independent (within limits) of the sensor orientation, they depend only on the feedback coils. JPL uses a triaxial coil system for their vector helium magnetometer, the frame is made from a single piece of plastic so that it tends to expand equally in all directions with temperature changes. Nearly all of the system presented in this report would be applicable to a system using triaxial feedback coils. If time permits under the present study contract, such a system will be further explored.

References

Gordon, D.I. and R.E. Brown, "Recent Advances in Fluxgate Magnetometry, IEEE Trans. Magn., vol. MAG-8, no. 1, March, 1972.

Scouten, D.C., "Sensor Noise in Low-Level Flux-Gate Magnetometers," IEEE Trans. Magn., vol. MAG-8, no. 2, June, 1972.

Power, James J., "A Digital Offset Fluxgate Magnetometer for Use in Remote Geomagnetic Observatories," Publ. No. 1247-37, Institute of Geophysics and Planetary Physics, UCLA, Sept. 1973.

Dobkin, Robert C., "On Chip Heater Helps to Stabilize Monolithic Reference Zener," Electronics, vol. 49, no. 19, Sept. 16, 1976.
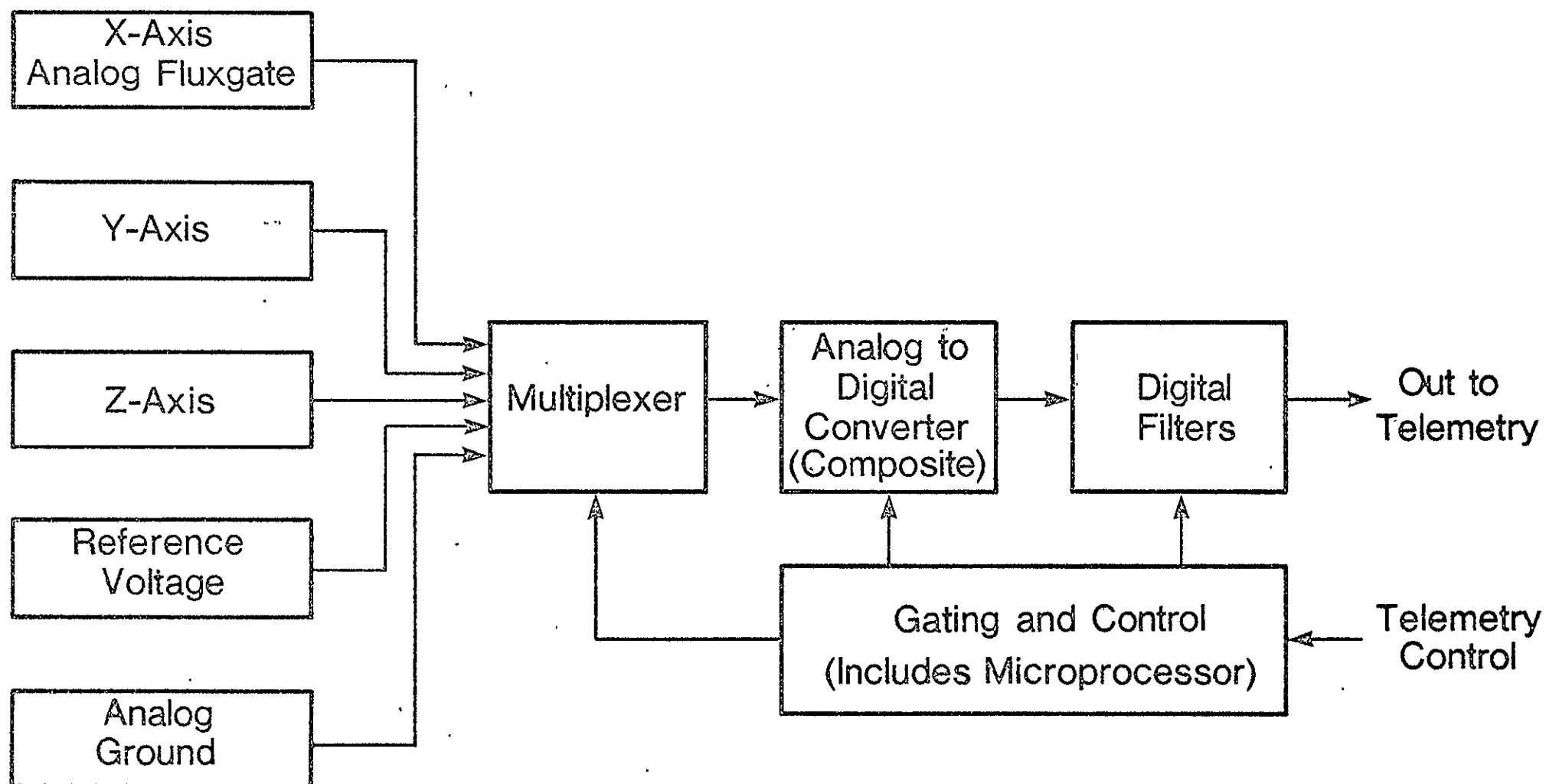
F I G U R E   1

System Diagram Tri-Axial Digital
Fluxgate Magnetometer
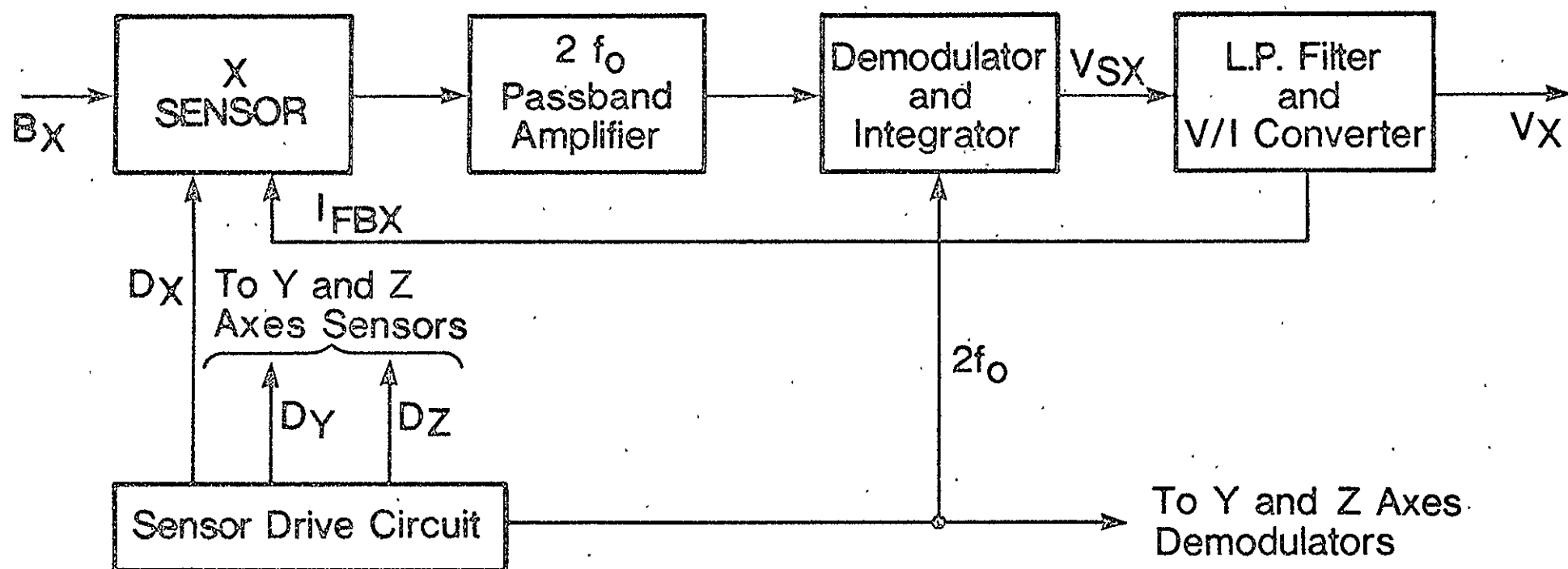
F I G U R E   2
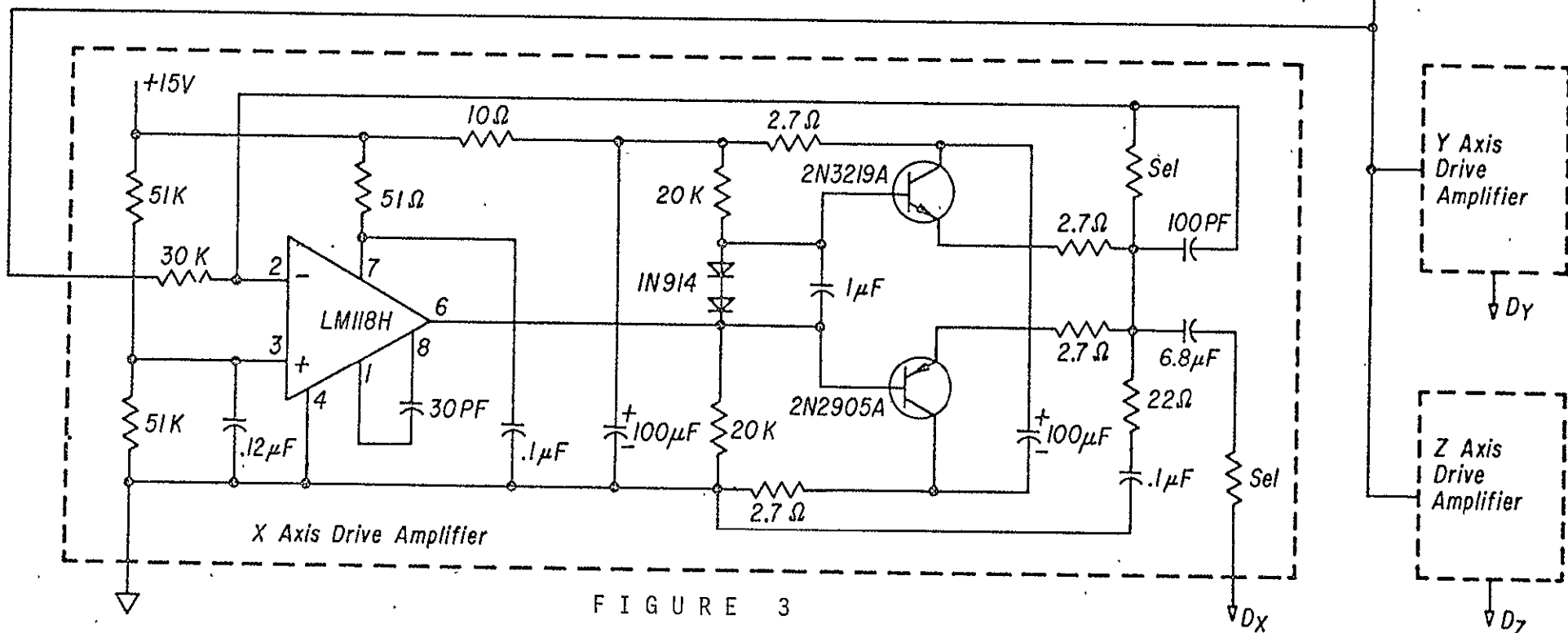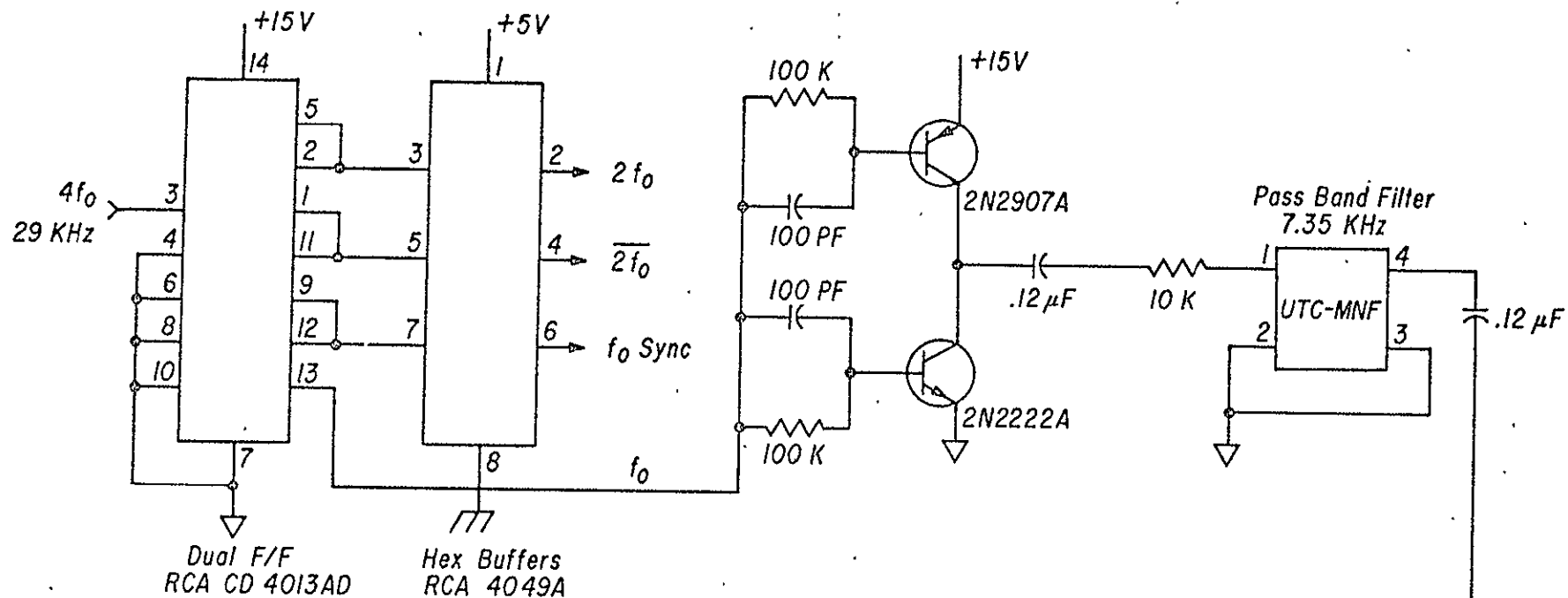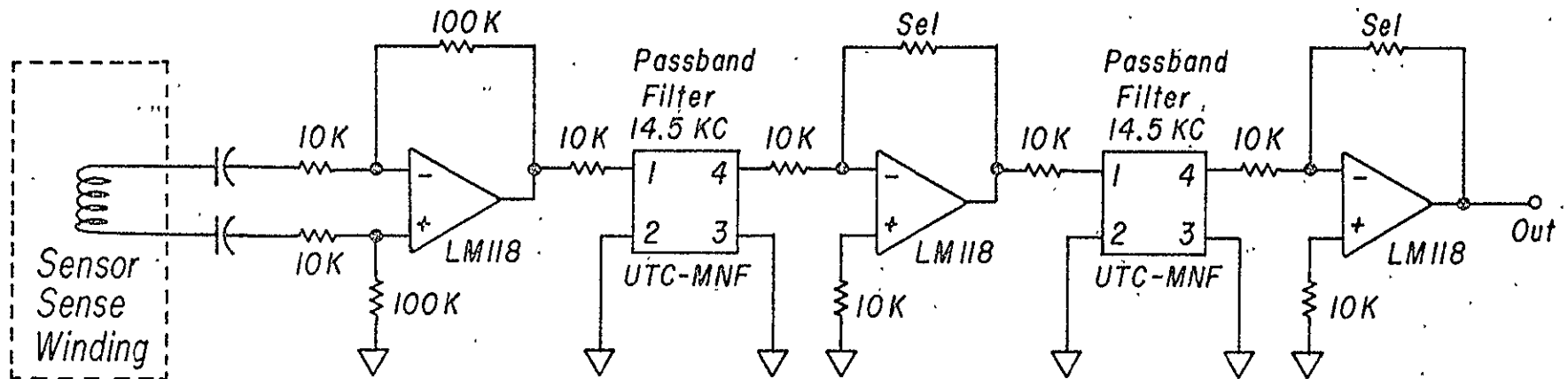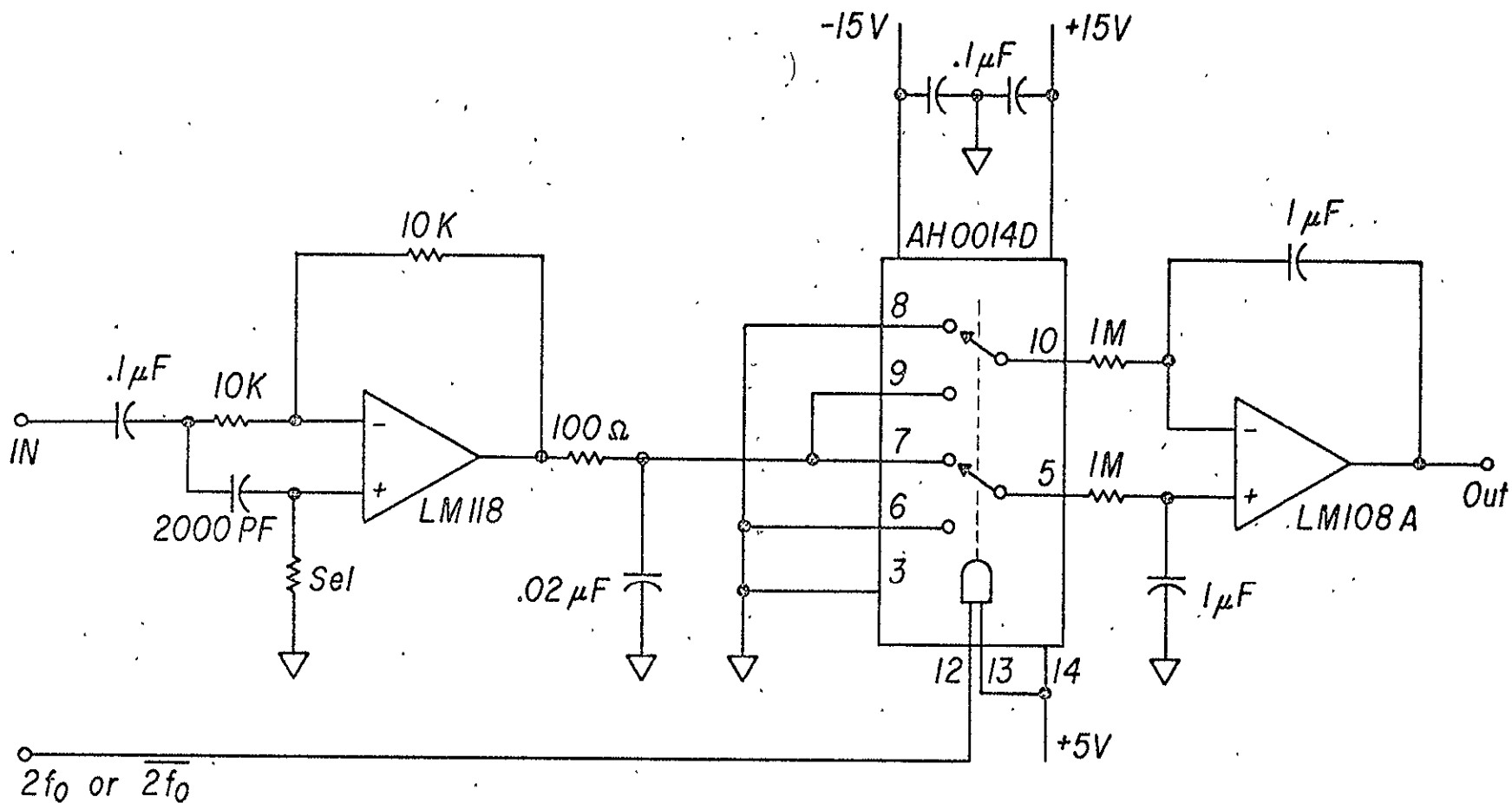
System Block Diagram Tri-Axial
Fluxgate Magnetometer

FIGURE 3

Sensor Drive Circuit

36

Note: Compensation and power supply connections not shown.
±15V Power supply
Feedback resistors chosen to adjust gain.

F I G U R E   4

$2f_o$ Passband Amplifier

Note: Compensation and ±15V power supply connections
not shown for OP amps.

FIGURE 5

Demodulator and Integrator
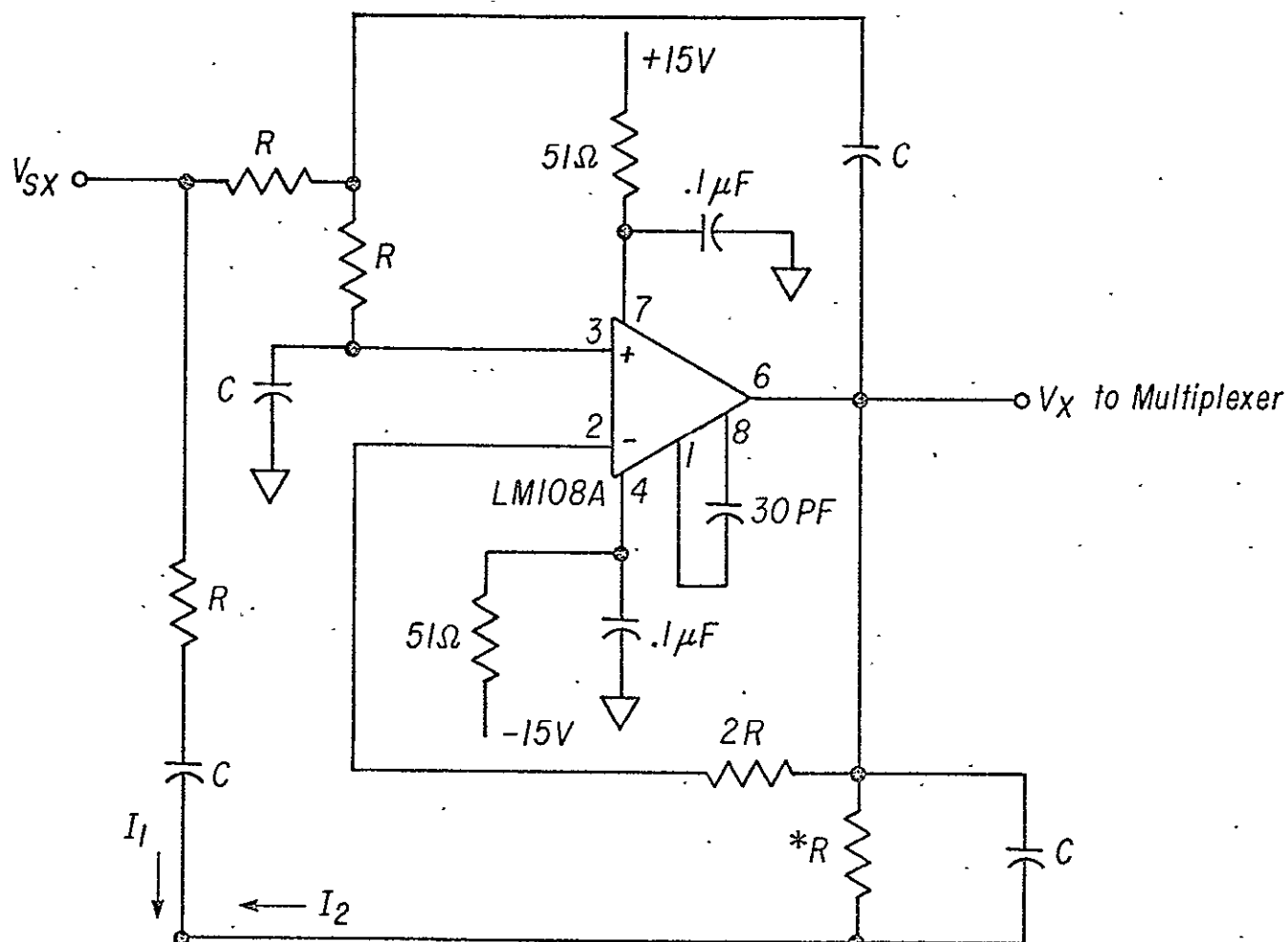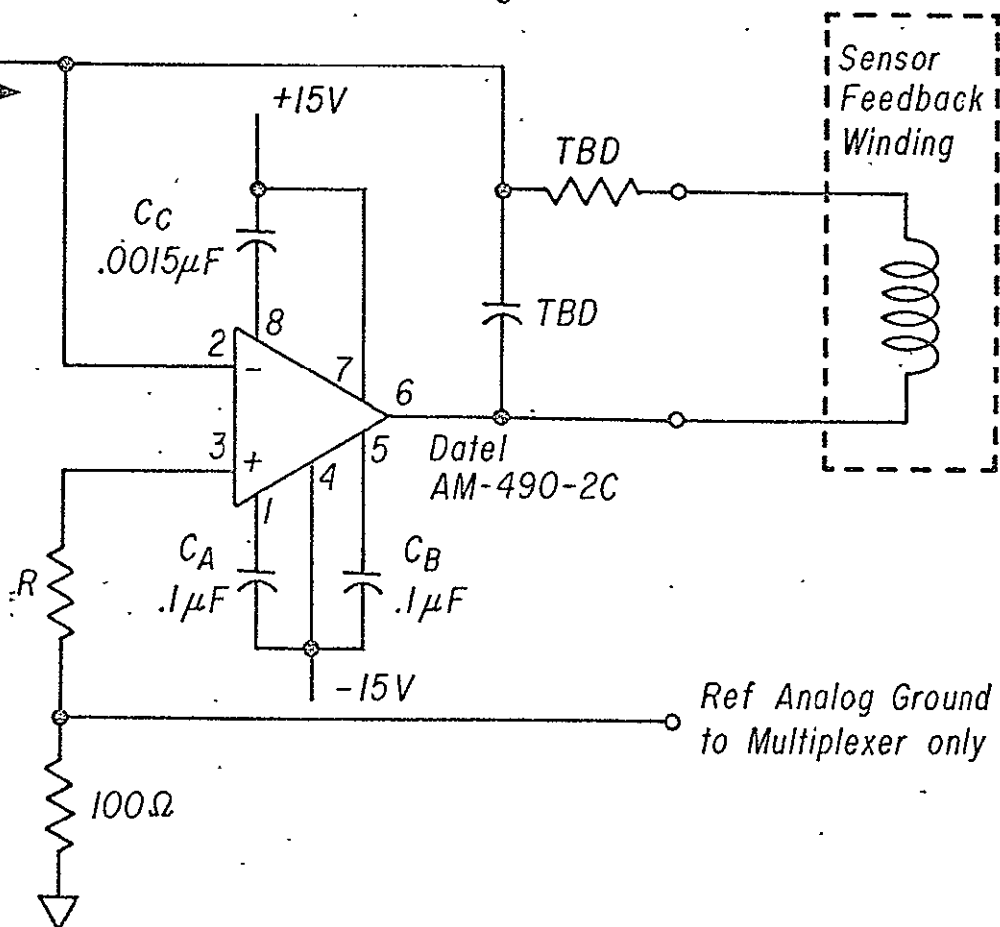
39

FIGURE 6
Lowpass Filter and V/I Converter

V_{SX}

R

R

C

$+15V$

51Ω

$.1\mu F$

C

3

7

+

6

V_X to Multiplexer

2

8

−

LM108A

4

51Ω

$.1\mu F$

30 PF

$-15V$

$2R$

*R

C

R

C

I_1

I_2

I_{FB}

$+15V$

C_C
$.0015\mu F$

8

2

−

7

6

3

+

5

Datel
AM-490-2C

TBD

TBD

Sensor
Feedback
Winding

C_A
$.1\mu F$

C_B
$.1\mu F$

R

4

1

$-15V$

100Ω

Ref Analog Ground
to Multiplexer only

Notes:
*Ultra stable resistor
$R = 10K$
$C = .5\mu F$
$V_X / V_{SX} = 1/(1+ST)^2$
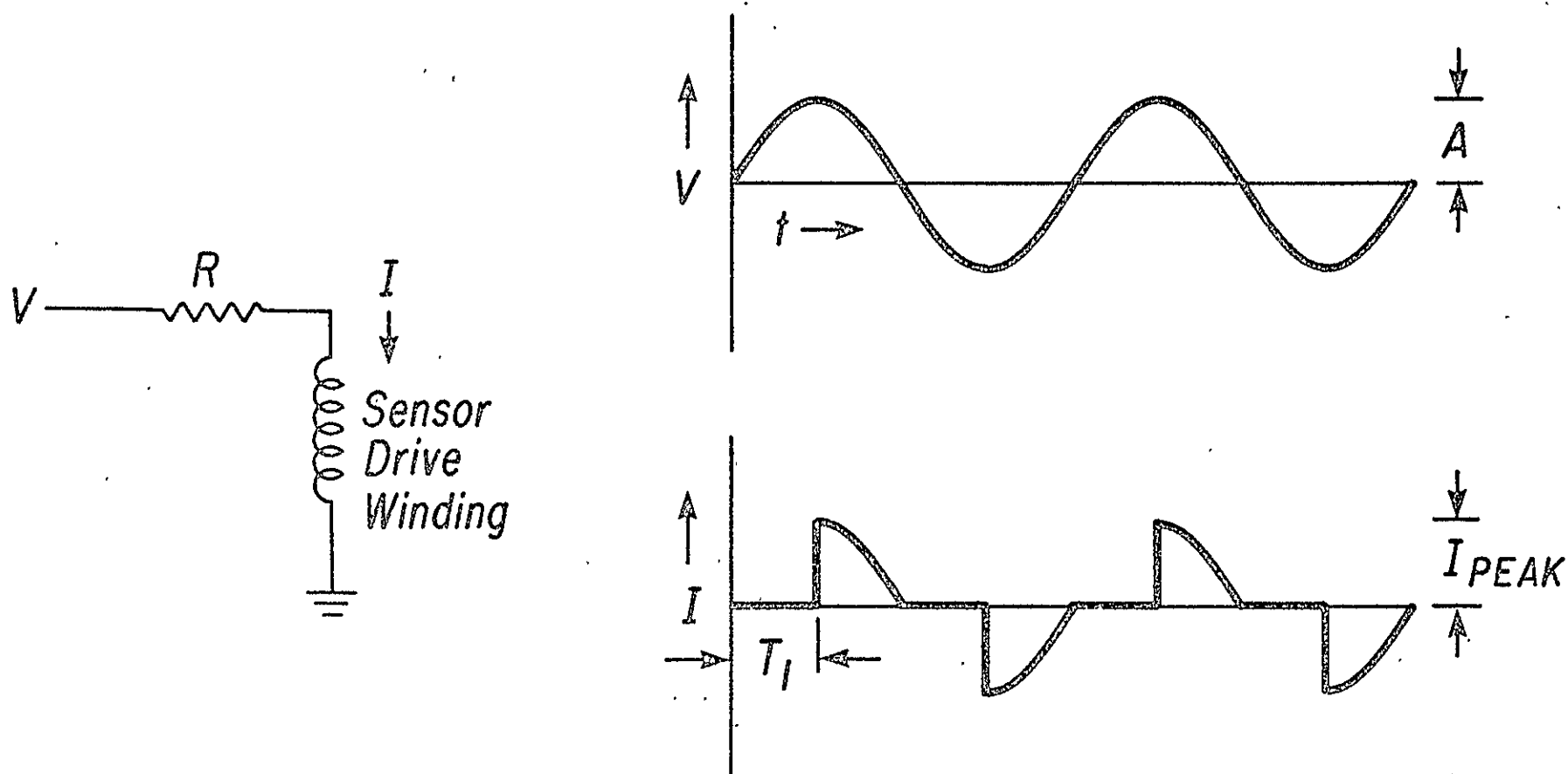Where $T = RC$
$1/(2\pi RC) \approx 30 Hz$

FIGURE 7

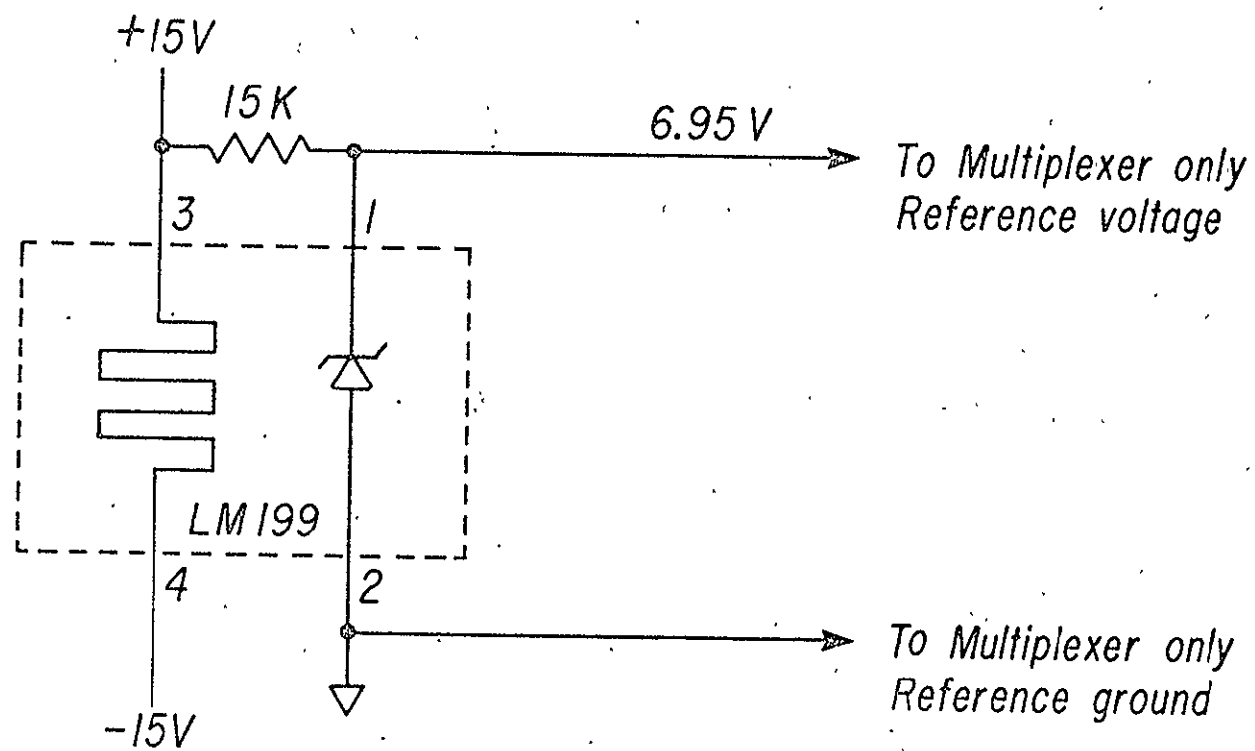Sensor Drive Winding Voltage and
Current Waveforms

FIGURE 8

Reference Voltage

A High Linearity, High Resolution, Analog to Digital Converter·

M.G. McLeod·

Introduction:

This report describes a method for producing a very highly linear analog
to digital converter which also possesses high resolution. The converter
is a composite. One of its elements is a successive approximation type
analog-to-digital converter. The composite will be referred to as the McLeod
·converter.

·The McLeod converter achieves its high linearity and high resolution
at the expense of a slow conversion speed relative to the successive
approximation converter. It is intended to be used in conjunction
with a multiplexer for the conversion to digital form of slowly varying
analog signals. If analog ground and a reference voltage are two of the
multiplexer inputs, the digital outputs corresponding to these two inputs
can be used to correct the digital outputs corresponding to the remaining
multiplexer inputs for zero and gain variations of the McLeod converter.
The complete system will have good gain and zero-stability, since the McLeod
converter is effectively "chopper stabilized."

The linearity and·resolution of the McLeod converter depend upon the
linearity and resolution of the successive approximation converter used and
upon the conversion speed of both the successive approximation converter
and the composite McLeod converter. For example, if the successive approxi-.
mation converter is a 12 bit converter with a linearity of $\pm$ 1/2 the least
significant bit and a conversion time of 10 microseconds, and if the McLeod
converter has a conversion time 256 times greater than the successive
approximation converter (2.56 milliseconds) then the McLeod converter will

The undersigned have read and understand the invention disclosed herein.

Inventor's signature _Malcolm G. M⁅ Leod_ Date _Oct 8, 1976_

Witness _____ Date _Oct 8, 1976_

Witness _Joseph D. Mears_ Date _Oct 8, 1976_

be a 19 bit converter with a linearity of ± 1/2 the least significant bit.
Thus linearity and resolution will be better than ± one part per million.
Time and temperature variations of the linearity of the McLeod converter
are also less than those of the successive approximation converter by the
same factor as the linearity itself is improved.

Description:

A schematic diagram of the McLeod converter is shown in Figure 1. A
basic element of this converter is a successive approximation type analog to
digital converter. (Other types of converters, such as a tracking converter,
could also be used.) A sample and hold prevents the input to the successive
approximation converter from changing during its conversion time. The
analog input being measured is applied to a voltage follower (operational
amplifier #1) whose output is one of the inputs to a summing amplifier
(operational amplifier #2). The other input to the summing amplifier is a
sawtooth voltage (more exactly, in the embodiment shown, it is a staircase
voltage) whose period is the conversion time of the McLeod converter. The
output of the summing amplifier is a sawtooth voltage superimposed upon
the signal being measured. We shall assume the voltage being measured is
substantially constant during the conversion time of the McLeod converter.
The amplitude of the sawtooth voltage at the input to the successive approxi-
mation converter is adjusted to be just slightly greater than one-half of
full scale for the successive approximation converter. This is discussed
further in the next section. For illustrative purposes, we shall take the
successive approximation converter to be a 12 bit converter with 10 microsecond

The undersigned have read and understand the invention disclosed herein.

Inventor's signature _Malcolm P. Mc Leod_ Date _Oct 8, 1976_
Witness _____ Date _____
Witness _Joseph N. Means_ Date _Oct 8, 1976_

conversion time and $\pm$ 10 volt, full scale input range. The sawtooth (or staircase) is generated by a 12 bit digital to analog converter with a $\pm$ 10 volt full scale output when used in conjunction with operational amplifier #3. Only the eight most significant bits are used, the staircase lasts for 256 conversion periods of the successive approximation converter. The 256 outputs of the successive approximation converter during one conversion of the McLeod converter are summed by a digital filter, this sum is the digital output of the McLeod converter for a single conversion.

Theory of Operation:

The calibration curve for the successive approximation converter is a plot of the digital output vs. the input voltage. Due to the inevitable presence of noise, the digital output for a constant input will vary from reading to reading, thus the average digital output is plotted, and the curve is continuous. In the absence of noise, the plot would (ideally) be a staircase, due to noise the corners of the staircase are rounded off. One can also make a plot of the deviation of the digital output from the best straight line as a function of input voltage. For an ideal converter, this plot would be a sawtooth waveform whose amplitude (peak-to-peak) is one least significant bit of the converter and whose period is the analog input voltage corresponding to one least significant bit. For a 12 bit converter, there will be 4096 cycles of the sawtooth over the full scale range of the input. For a non-ideal converter, the edges of the sawtooth will be rounded because of the presence of noise. Furthermore, there will in general be "bit error nonlinearities." If the most significant bit is in error, there will be in

The undersigned have read and understand the invention disclosed herein.

Inventor's signature _Malcolm D. McLeod_ Date _Oct 8, 1976_

Witness _____ Date _Oct 8, 1976_

Witness _Joseph D. Means_ Date _Oct 8, 1976_

addition a sawtooth of amplitude equal to the bit error and having two cycles

over the full scale range of the input voltage, if the next most significant

bit is in error the corresponding sawtooth will have four cycles over the

range of the input voltage, etc. Thus the plot of deviation from linearity

vs. input voltage will consist of the sum of a number of sawtooth waveforms,

the number of cycles of each waveform over the input range will be a power

of two. This is the deviation from linearity due to "bit error nonlinearities."

These nonlinearities are the dominant nonlinearities for many successive

approximation converters. Let us now consider the calibration curve for

the McLeod converter. Initially, let us suppose that the conversion time

for the successive approximation converter is infinitesimal, that there are

an infinite number of successive approximation conversion periods during one

McLeod converter conversion, and that the staircase output from the digital

to analog converter is a ramp. Then the calibration curve for the McLeod

converter is obtained from the calibration curve of the successive approxi-

mation converter by averaging this calibration curve over an interval centered

at the input voltage and of width equal to one-half of full scale. This

averaging process is a filter, all of the sawtooth waveforms of the deviation

from linearity plot are filtered out by this filter which has notches at all

the sawtooth frequencies. Only one-half of the input range of the successive

approximation converter is available for the input signal since one-half

of the range is used for the ramp. For this idealization, the McLeod

converter is perfectly linear (neglecting second order effects). During

The undersigned have read and understand the invention disclosed herein.

Inventor's signature _Malcolm D. McLeod_ Date _Oct 8, 1976_

Witness _____ Date _Oct 8, 1976_

Witness _Joseph A. Means_ Date _Oct 8, 1976_

a single conversion of the McLeod converter, each of the bits in the successive approximation converter is "on" one-half of the time except for the most significant bit which is "on" for a duration linearly related to the input signal. The preceding discussion assumes that the ramp amplitude is exactly one-half of the range of the successive approximation converter.

For an actual McLeod converter with a finite number of steps (in our example, 256) to the ramp (or staircase) and a finite conversion time for the successive approximation converter, the number of times the most significant bit is "on" during a complete conversion will be an integer between 0 and 255, thus the maximum error due to errors in this bit will not be zero but will be reduced by a factor of 256. Since full-scale is reduced by a factor of two, the linearity is thus improved by a factor of 128 compared to the successive approximation converter.

Finally, let us consider the resolution of the McLeod converter. If the steps of the staircase at the input to the successive approximation converter are an integral multiple of the step size for the successive approximation converter, then the resolution of the McLeod converter is the same as that of the successive approximation converter, since for a constant analog input all of the inputs to the successive approximation converter will occupy the same relative positions within the digital "windows." If, however, the amplitude of the staircase is adjusted to a value slightly greater than one-half of full scale, so that 256 windows of the digital to analog converter as measured at the input to the successive approximation converter exceed the 2048 windows of the successive approximation converter

The undersigned have read and understand the invention disclosed herein.

Inventor's signature _Malcolm B. McLeod_ Date _Oct 8, 1976_

Witness _____ Date _Oct 8, 1976_

Witness _Joseph D. Mems_ Date _Oct 8, 1976_

corresponding to half of full scale by an odd number of windows (say 5),
then the input to the successive approximation converter will be evenly
distributed within its digital windows, and the resolution of the McLeod
converter will be 128 times greater than that of the successive approximation
converter. It might seem at first that the digitization noise is reduced
by a larger factor than is possible. For a random digitization error, the
digitization noise is only reduced by the square root of the number of
samples, in this case 16. However, the digitization error for each conversion
is not random but is evenly distributed throughout the window for a
complete conversion of the McLeod converter. Thus the McLeod converter
increases the resolution by a factor greater than 16. If there is noise
present in the successive approximation converter in addition to the
digitization noise, this noise will be reduced by a factor of eight.

. It is apparent from our discussion thus far that the averaging action
of the McLeod converter will also reduce other nonlinearities than those of
the "bit error" type, being most effective for nonlinearities that have
a high frequency on the plot of deviation from linearity vs. input voltage.
This includes nonlinearities that result from finite settling times of the
components of the successive approximation converter.

Choice of Components:

At the present time (September, 1976) there are three types of successive
approximation converters that might be considered for use in the McLeod
converter. These are monolithic, hybrid, and discrete component types.

The undersigned have read and understand the invention disclosed herein.

Inventor's signature _Malcolm D. McLeod_ Date Oct 8, 1976

Witness _____ Date Oct 8, 1976

Witness _Joseph V. Menns_ Date Oct 8, 1976

(References 1 and 2). The best converters use discrete components, such as Intech's A-856-16, which is a 16 bit converter with a 8 microsecond conversion time. These are relatively expensive ($1,300) and are not commercially available to military specifications. It would be possible to build one to meet such specifications using the approach described in reference 3. Among other things, extremely stable resistors are required. Monolithic converters appear to offer no advantages over hybrid except for lower cost. Two chip hybrid analog to digital converters having 12 bits and 12 microsecond conversion speeds should be obtainable for less than $20 by early 1978 (reference 2).

The best currently available hybrid analog to digital converter appears to be Burr Brown model ADC 85. This is a 12 bit converter with a ten microsecond conversion speed and sells for $225. It is faster than competitive products. A suitable digital to analog converter is Burr Brown model DAC 85 which has 12 bits and a 300 nanosecond settling time. It sells for $89. Suitable operational amplifiers are Burr Brown model 3550 K which have 600 nanosecond maximum settling times and sell for $27. A suitable sample and hold would be Burr Brown model SHC 85 which sells for $65. This would increase the total conversion time somewhat (less than 50%). It is possible that the sample and hold would not be necessary in some applications.

With the components indicated, the McLeod converter will be a 19 bit converter with linearity of ± 1/2 the least significant bit. By using a discrete component successive approximation converter and a longer conversion time, it should be possible to improve its performance by as much as 6 bits.

The undersigned have read and understand the invention disclosed herein.

Inventor's signature _Malcolm D. McLeod_ Date _Oct 8, 1976_

Witness _____ Date _Oct 8, 1976_

Witness _Joseph A. Means_ Date _Oct 8, 1976_

References

1. "Digital Converters: Changing the Real World," Evanzia, W.J., <u>Electronic Products</u>, p. 23, December, 1975.

2. "Success Springs from Innovation," Gadway, R., <u>Electronic Products</u>, p. 53, June 1976.

3. "Design a Precision a/d Converter," Marosi, G., <u>Electronic Design</u>, p. 66, Vol. 23, no. 8, April 12, 1975.

1000 pF

5K

Analog in o——
(From Multiplexer)

OP Amp #1

10 K

OP Amp #2

S/H

ADC

Out o——
(To Digital Filter)

DAC

OP Amp #3

10 K

Gating and Control

To Multiplexer
To Digital Filter
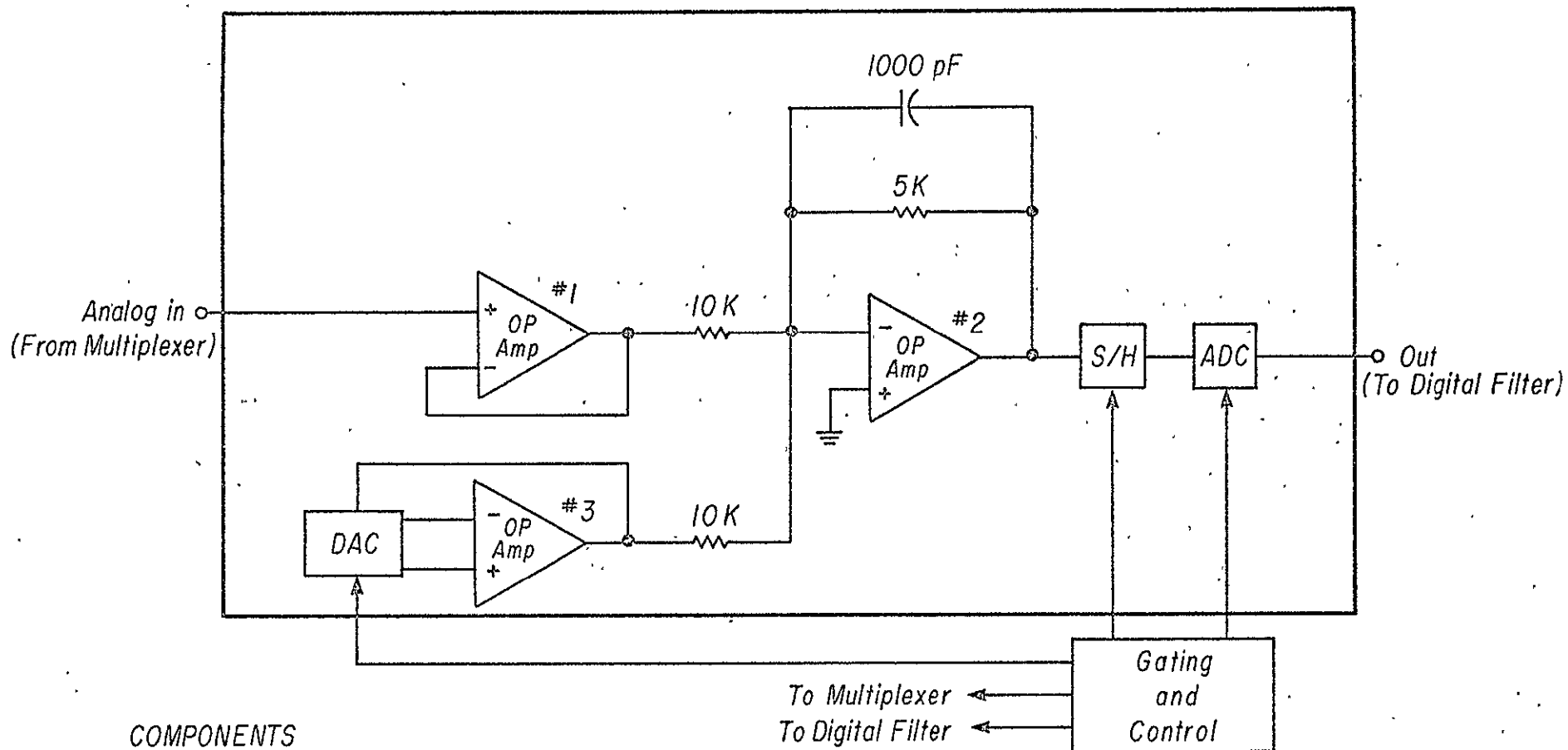
COMPONENTS

DAC   Digital to Analog Converter
S/H   Sample and Hold
ADC   Analog to Digital Converter
       (Successive Approximation)

The undersigned have read and understand the invention disclosed herein:

Inventor's signature: _Malcolm S. McLeod_ Date: _Oct. 8, 1976_

Witness: _____ Date: _Oct 8, 1976_

Witness: _Joseph O. Means_ _____ Date: _Oct 8, 1976_

Figure 1

Schematic Diagram
McLeod Analog to Digital Converter

Limitations of Triaxial Digital Fluxgate Magnetometers

The limitations of digital fluxgate magnetometers can be subdivided into two categories:

(a) The limitations of an analog output fluxgate magnetometer.

(b) The limitations of an analog to digital converter.

Analog fluxgate magnetometers can be subdivided into two categories:

(a) Elementary fluxgate magnetometers where a sensor detects a field along its magnetic axis as an AC signal which is then amplified and detected as a DC signal.

(b) Those using a feedback coil about the sensor. The coil is driven by the output of an elementary fluxgate magnetometer to provide negative field feedback.

Triaxial analog fluxgate magnetometers using field feedback can be further subdivided into two categories:

(a) Those for which the three orthogonal axes operate independently of one another (ideally).

(b) Those for which all three sensors are within a single set of orthogonal feedback coils, so that the feedback mechanism operates to tend to null all three components of the field at each sensor.

The use of field feedback tends to make the transfer function relating magnetometer output to a magnetic field component independent of the sensor and electronics gain and nonlinearities, and strongly dependent on the transfer function of the feedback path, in particular the feedback coil and any resistor that might be used to convert a magnetometer output voltage to a current through the coil. For a single axis magnetometer, the magnetic axis direction is

determined by the sensor orientation, and the orientation of the feedback coil relative to the sensor is involved in the feedback transfer function. When all three sensors are within a single set of feedback coils, then it is the coils that determine the magnetic axes of the magnetometer, largely independent (within limits) of the sensors' orientations and gains.

Because the transfer function associated with a feedback coil is more linear and can be made much more stable with time and temperature then the transfer function associated with the sensor and electronics, only fluxgate magnetometers using the field feedback principle should be considered as candidates for a highly stable fluxgate magnetometer.

Because the sensor output does not depend only on the field at a mathematical point, but on the weighted average of the field over a volume in space, and because the feedback coil does not produce a uniform field over all space, any dependence of the sensor weighting function on magnetic field will be reflected in the feedback transfer function, and will produce nonlinearities in the closed loop transfer function of the magnetometer. Moreover any dependence of the sensor weighting function on time or temperature will also be reflected in the feedback transfer function, and thus in the closed loop transfer function of the instrument, even in the limit where the open loop gain becomes infinite. These nonlinearities and time and temperature dependencies can be reduced by the use of a sufficiently large feedback coil or one which produces a sufficiently uniform field over a sufficiently large volume.

It is clear also that the feedback transfer function will reflect variations in orientation, position, or size of the feedback coils due to time

or temperature, and in the case of a single axis feedback system, orientation of the sensor will also be involved.

An elementary fluxgate magnetometer (open loop) will also exhibit an output that is not determined by the ambient magnetic field. This output is referred to as offset, drift, or noise according to whether it is DC, low frequency, or higher frequency. No universal agreement exists concerning the frequency boundaries. Perhaps frequencies above .001 Hz might be considered as noise, and those below 1 cycle per year might be considered offset. We shall refer to them all as noise. It is important to realize that noise (referred to the input, i.e., expressed in magnetic field units) is not reduced by the use of field feedback. There are numerous sources of noise in a fluxgate magnetometer. Since the sensor is driven at a drive frequency f_0 and the second harmonic of this frequency $2 f_0$ is detected as a measure of the magnetic field, harmonic distortion due to nonlinearities in the drive circuit can produce noise. Since the detected signal contains a large amount of fundamental, nonlinearities in the amplifiers of the detection circuitry can produce noise. Since the second harmonic frequency is also generated by the instrument and used for phase sensitive demodulation of the detected second harmonic, it also is possible for noise to be produced in the detection circuitry through power supply interactions or capacity coupling. Noise is also produced in the sensor primarily due to departures of the geometry and magnetic properties from an ideal model, and this noise can be both electro- statically and electromagnetically coupled to the secondary and detected. The amount of noise is dependent also on the drive waveform and amplitude. Any of

these noise sources might be dominant in a particular fluxgate magnetometer, depending on the care used in its design and construction. In general, some of these noise sources may be field (or output) dependent, particularly in a complete instrument including an analog to digital converter, so it is important to measure noise not only in zero ambient field but also the largest field expected to be encountered and various field orientations.

Next, we shall look at the limitations of an analog to digital converter. There are essentially three methods of analog to digital conversion, with variations on these methods. The three methods are:

(a) Parallel converter

(b) Integrating converter

(c) Feedback systems using digital to analog converters

The parallel converter involves a resistor divider and a number of level detectors to separate the input signal into a number of windows. Usually, the number of windows is small (less than 16) since a large number of components is required for a large number of windows. Each window can be further subdivided by schemes involving switches and another parallel converter. The main virtue of this method is that it can be very fast, its chief limitation is in the accuracy required of the level detectors and the resistor divider. This method has not been used for high resolution converters.

The integrating type converter involves charging a capacitor with a current proportional to the input (referred to ground) for a predetermined time, then discharging it with a current having the same proportionality to a (negative) reference voltage until the capacitor reaches ground potential.

The time required for discharge is measured, the ratio of the two times is the ratio of the input voltage to the reference voltage. The main virtue of this system is excellent differential linearity and the fact that the digital output is independent of the resistor and capacitor used, provided the same resistor is used for both charge and discharge. One limitation is that it is relatively slow when high resolution is desired, since it is difficult with present techniques to use clocks having higher frequency than about 10 MHz. Some integrating type converters have an automatic zero correcting feature; however, such a feature is not inherent in the conversion method and can be incorporated into any conversion method. Another advantage of the integrating converter is the noise filtering achieved by the integration. Since a major effort in analog to digital conversion has been directed toward achievement of high conversion speeds, the integrating type converter has probably not been developed to its highest potential.

Finally, we come to methods involving the use of digital to analog converters in feedback systems. There are two basic methods that can be used, with variations upon them:

(a) Tracking converters

(b) Successive approximation converters

In the tracking converter, the difference between the output of the D/A converter and the analog signal being measured is amplified and used to operate a level detector. Periodically the output of the level detector is examined, if positive the digital input to the D/A converter is decreased one unit, if negative the digital input is increased one unit (or vice-versa, depending on whether or not the amplifier is inverting). The digital output tracks the analog input, but is slew rate limited, i.e. the digital output can not change by more than one unit per sample period.

The successive approximation converter also works by comparing the D/A output with the signal being measured and using this information to change the D/A digital input. The bits of the D/A converter are turned on in succession starting with the most significant bit, after each bit is turned on it is left on if the D/A output is less than the analog input and it is turned off if the contrary is true. Thus the final D/A digital output will be less than one bit below the analog input. The advantages of the successive approximation method is that it is not slew rate limited like the tracking converter, the disadvantage is that the analog input must remain constant within one bit during a conversion period to avoid serious errors. This is usually accomplished by the use of a sample and hold which measures the analog input during a short time period and then provides a constant output (ideally) to the A/D converter during the conversion cycle.

When used with a fluxgate magnetometer having field feedback, the magnetometer can be used as the difference sensing element of the converter, i.e., the D/A converter output can be applied to the feedback coil, the difference between the ambient field and the feedback field sensed by the magnetometer, and this difference used to vary the digital input to the D/A converter. This scheme is not practical for a successive approximation type converter, as there is no practical way to sample and hold the ambient magnetic field. This scheme (or a variation of it) has been used with tracking type fluxgate magneto-meters. At one time (during the 1960's) it was the best way to build a highly stable fluxgate magnetometer, fundamentally because a magnetic amplifier was the best way (less noise and offset) to detect small currents. With the advent

of FET op amps and switches having extremely low leakage currents, this is no longer the case, and there is no longer any fundamental reason from a performance point of view to put the D/A converter in the feedback loop of the fluxgate magnetometer. Since the response time of a fluxgate magnetometer is considerably longer than what can easily be achieved with semiconductor amplifiers, a faster slew rate can be achieved with the converter out of the loop. It should be mentioned here that an analog fluxgate magnetometer using field feedback and having an integrator in the forward section of the loop (the best kind) is itself slew rate limited, but putting the converter in the loop can limit it further.

All of the analog to digital converters mentioned contain:

(a) A reference voltage

(b) Switches, difference amplifiers, and/or level detectors

(c) A clock and/or a resistor network. (Conceptually, other components could be used in place of resistors.)

Thus all of the analog to digital converters are subject to the limitations of some or all of these devices.

Only the use of a field feedback type fluxgate magnetometer in conjunction with an A/D converter that utilizes a D/A converter with a feedback system have been considered here as suitable candidates for a high-resolution high-stability triaxial fluxgate magnetometer, although an integrating type A/D converter could possibly be used.

Summarizing, some of the necessary limitations of the type system considered here are the variations with time and temperature of:

1. Sensor offset

2. System gain, due to variations of

    (a) The reference voltage
    (b) The resistor (or resistors) used to convert the reference
         voltage to a current through the feedback coil
    (c) Coil and/or sensor geometry
    (d) Sensor weighting function

Another limitation is the system linearity and its variations with time and temperature. Nonlinearities are due to:

.1. Sensor, because of dependence of weighting function on magnetic field.

2. The analog to digital conversion. These nonlinearities are mainly due to limitations in the trimming and tracking of the resistors in the divider networks associated with digital to analog converters.

Finally, offset and gain variations associated with the analog electronics and analog to digital conversion can be important. Their importance will depend upon the particular system and circuit design.

Numerical Values:

1. Sensor offset: For the NOL sensors it is about .7 gamma. Its Tempco is 3 milligamma/°C. We do not have data for the time variations of the offset. Some experiments conducted at UCLA indicate that the offset (and noise) can probably be reduced by an unknown amount by the use of an electrostatic shield between the primary and secondary windings.

2. Reference voltage: Motorola reference diodes type MZ 605 have stabilities better than 5 ppm/1000 hr. Assuming a random walk type drift, this would correspond to 15 ppm/yr. Temperature stability can be adjusted

to about 1 ppm/°C by adjusting the current through the diode. As these units are listed in Motorola's 1968 Handbook, possibly better units may now be available.

3. Resistors: The best resistors available (other than lab standards) are ultra precision resistors manufactured by Vishay Corp. They.are stable to 5 ppm/yr. and have temperature coefficients of 1 ppm/°C. Thin film resistor networks such as are used in many digital to analog converters track to within 1 ppm/°C but have individual temperature coefficients of about 25 ppm/°C. These networks track with time to about 100 ppm/yr.

4. Sensor gain: We do not have data on sensor gain variations due to variations with time or temperature of coil and/or sensor geometry or sensor weighting function.

5. Sensor linearity: Measurements made at UCLA indicate that the NOL sensor linearity is better than 4 gamma out of 40,000. This figure represents the limitation of the measurement, not the sensor. Measurements made on other sensors have shown nonlinearities as much as 100 gamma out of 64,000.

6. Analog to digital converter linearity: 12 bit hybrid types are available with linearities better than $\pm$ 1/2 least significant bit. For full scale of $\pm$ 64,000 gamma, this corresponds to $\pm$ 8 gamma, or $\pm$ 125 ppm of full scale.